

**Hydrothermal Synthesis of Carbon Nanodots from
Pectinodesmus sp. for Drug Delivery via Chitosan
Hydrogels**



Submitted by

Arooj Fatima (357689)

Mudassar Iqbal (357436)

Saif ul Eman (357927)

Supervised by

Dr. Hussnain Ahmad Janjua

Atta-Ur-Rahman School of Applied Biosciences (ASAB)

National University of Sciences & Technology (NUST)

(2024)

THESIS ACCEPTANCE CERTIFICATE

It is certified that the final copy of the BS FYP Thesis titled “Hydrothermal Synthesis of Carbon Nanodots from *Pectinodesmus sp.* for Drug Delivery via Chitosan Hydrogels” submitted by Arooj Fatima, Mudassar Iqbal and Saif ul Eman of ASAB, NUST have been vetted by the undersigned, found complete in all respects as per NUST regulations and have been found satisfactory for the requirement of the degree.

Signature (Supervisor):

Dr. Hussnain Ahmed Janjua

ASAB, NUST

Date:

Signature (HOD):

Dr. Fazal Adnan

ASAB, NUST

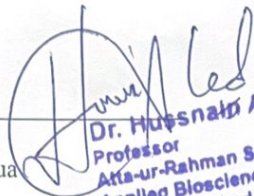
Date:

Signature (Dean/Principal)


Dr. Muhammad Asghar

ASAB, NUST

Date:


Dr. Hussnain A. Janjua
Professor
Atta-ur-Rahman School of
Applied Biosciences (ASAB)
NUST, Islamabad


Dr. Fazal Adnan
Head of Department (HoD)
Dept of Industrial Biotechnology
Atta-ur-Rahman School of Applied
Biosciences (ASAB), NUST Islamabad


Prof. Dr. Muhammad Asghar
Principal
Atta-ur-Rahman School of Applied
Biosciences (ASAB), NUST Islamabad

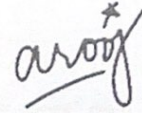
AUTHOR'S DECLARATION

We, Arooj Fatima, Mudassar Iqbal and Saif ul Eman hereby state that our BS FYP thesis titled "**Hydrothermal Synthesis of Carbon Nanodots from *Pectinodesmus sp.* for Drug Delivery via Chitosan Hydrogels**" is our work and has not been submitted previously by us for taking any degree from the National University of Science and Technology (NUST) or anywhere else in the country/world.

At any time if our statement is found to be incorrect even after our graduation, the university has the right to withdraw our BS degree.

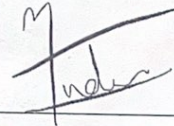
Name of student: Arooj Fatima

Signature



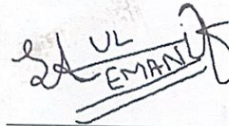
Name of student: Mudassar Iqbal

Signature



Name of student: Saif ul Eman

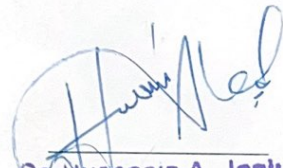
Signature



CERTIFICATE FOR PLAGIARISM

It is to confirm that this BS thesis titled “**Hydrothermal Synthesis of Carbon Nanodots from *Pectinodesmus sp.* for Drug Delivery via Chitosan Hydrogels**” by Arooj Fatima (357689), Mudassar Iqbal (357436) and Saif ul Eman (357927) has been examined by me. I undertake that,

1. The thesis has significant new work/knowledge as compared to already been published elsewhere. No sentence, table, equation, diagram, paragraph, or section has been copied verbatim from previous work except when placed under quotation marks and duly referenced.
2. The work presented is original and own work of authors i.e., there is no plagiarism. No idea, results, or works of others have been presented as the authors’ own work. There is no fabrication of data or results such that the research is not accurately represented in the records. The thesis has been checked using Turnitin, and a copy of the originality report is attached and focused within limits as per HEC plagiarism policy and instructions.



Dr. Hussnain A. Janjua
Professor (Supervisor)
Atta-ur-Rahman School of
Applied Biosciences (ASAB)
Dr. Hussnain Ahmad Janjua

Associate Professor

ASAB, NUST

*Dedicated to our exceptional parents,
teachers, friends, and adored siblings
whose tremendous support and
cooperation led us to this wonderful
accomplishment!*

ACKNOWLEDGEMENTS

In the name of Allah, the Most Gracious, the Most Merciful.

Alhamdulillah, all praise, and thanks to Allah Almighty, the Lord of the Worlds. It is with a profound sense of gratitude that we acknowledge His infinite blessings and guidance throughout our academic journey and the completion of this thesis.

We are deeply grateful to Allah for bestowing upon us the intellect, determination, and perseverance to undertake this research endeavor. His mercy and blessings have been a constant source of inspiration and strength, enabling us to navigate the challenges and complexities of the research process.

We would like to thank our principal Dr. Muhammad Asghar for providing us with this opportunity, and our supervisor Dr. Hussain Janjua who continued to be a form of support, care, and backing to us in times of uncertainty throughout the various phases of our final year project. His trust in our abilities made us work on this project confidently. Accept our heartfelt gratitude for your time, support, and patience.

We would like to take this opportunity to express our deepest gratitude and appreciation to our family and friends who have supported us throughout our academic journey and the completion of this thesis. Their unwavering encouragement, love, and understanding have been invaluable to us, and we are truly blessed to have such incredible individuals in our lives.

Most importantly, we would like to appreciate and acknowledge the countless hours our seniors Ms. Noor Fatima, Ms. Shafia Maryam, and Ms. Mishal Amjad, have dedicated to proofreading our work, providing feedback, and offering valuable insights. Their attention to detail, constructive criticism, and suggestions have played a significant role in refining our thesis and enhancing its quality. Their input and perspectives have broadened our horizons and shaped our research in ways we could not have accomplished alone.

We would also like to acknowledge School of Chemical and Materials Engineering (SCME), NUST; Nanotechnology Lab, School of Interdisciplinary Engineering & Sciences (SINES), NUST; Advanced Energy Materials and Systems Lab, USPCAS-E, National University of Sciences and Technology (NUST) for aiding in our research project.

We are grateful to Ms. Hina (ASAB) for her cooperation during the research project.

Finally, we would like to express our gratitude to all the individuals who have rendered valuable assistance to our final-year project.

As I conclude this acknowledgment, I am reminded of the verse from the Quran (Surah An-Nahl, 16:78), which states: "And Allah has extracted you from the wombs of your mothers not knowing a thing, and He made for you hearing and vision and intellect that perhaps you would be grateful." May Allah accept our humble efforts and make this thesis a means of benefit for others. All praise and thanks are due to Allah alone, the Lord of all creations.

TABLE OF CONTENTS

THESIS ACCEPTANCE CERTIFICATE	ii
AUTHOR'S DECLARATION	iii
CERTIFICATE FOR PLAGIARISM.....	iv
ACKNOWLEDGEMENTS	vi
LIST OF ABBREVIATIONS:.....	xii
ABSTRACT:.....	xiii
INTRODUCTION	1
1.1 Carbon Nanodots:	1
1.2 Hydrogels:.....	2
1.3 Drug Delivery System:	3
LITERATURE REVIEW	5
2.1 Carbon nanodots Discovery:.....	5
2.2 Synthesis of carbon:	5
2.2.1 Top-Down Approaches for Synthesis of Carbon Nanodots:	6
2.2.1.1 Laser Ablation:.....	6
2.2.1.2 Electrochemical Carbonization:.....	6
2.2.1.3 Exfoliation of Carbon Soot:	6
2.2.2 Bottom-up Approaches for Synthesis of Carbon nanodots:	7
2.3.2.1 Pyrolysis:.....	7
2.3.2.2 Microwave Assisted Approach:	7
2.3.2.3 Hydrothermal Method:.....	8
2.2 Carbon dots incorporation into Chitosan Hydrogel:	8
2.3 Drug Delivery properties of CQD:	8
MATERIALS AND METHODS.....	11
3.1 Hydrothermal Synthesis of Carbon nanodots:	11
3.2 Chitosan Hydrogel Formation:	12
3.3 Graphical Methodology:	14
3.3.1 Synthesis of Carbon Nanodots:.....	14
3.3.2 Formation of Chitosan Hydrogel:	14
3.4 Characterization of Carbon Nanodots:.....	15
3.4.1 Scanning electron microscopy (SEM):	15
3.4.1.1 Sample Preparation:	15

3.4.2 Energy Dispersive X-ray Spectroscopy (EDX or EDS):	15
3.4.2.1 Sample Preparation:	15
3.4.3 Fourier Transform Infrared Spectroscopy (FTIR):	15
3.4.3.1 Sample Preparation:	15
3.4.4 X-ray Diffraction Spectroscopy:	16
3.4.4.1 Sample Preparation:	16
3.4.5 UV-Vis Analysis:	16
3.4.5.1 Sample Preparation:	16
3.4.5 Antibacterial Assay:	16
3.4.5.1 Bacterial Growth:	16
3.4.5.2 Growth of <i>S. aureus</i> and <i>E. coli</i> :	16
3.4.5.3 Disk Diffusion Method:	17
3.4.6 Swelling and Degradation Studies:	17
3.4.7 Drug delivery studies:	17
3.4.7.1 Drug Loading (%):	17
3.4.7.2 In-vitro Drug Release Studies:	18
3.4.7.3 Standard calibration curve for drug release profile:	18
RESULTS:	19
4.1 SEM Analysis of (PHM3) Carbon Nanodots:	19
4.2 EDX Results of (PHM3) Carbon Nanodots:	20
4.3 FTIR Analysis of (PHM3) Carbon Nanodots:	20
4.4 XRD Analysis of CA (PHM3 algae) nanodots:	22
4.5 UV- Vis Spectrophotometry of PHM3 algae carbon nanodots:	23
4.6 Antibacterial Assay:	23
4.6.1 Antibacterial Activity Against <i>E. coli</i> :	24
4.6.2 Antibacterial Activity Against <i>S. aureus</i> :	25
4.7 Swelling and Degradation Studies:	26
4.8 Drug Delivery Studies:	27
4.8.1 Drug Loading (%):	27
4.8.2 Standard Curve of Vancomycin:	28
4.8.3 Drug release profile at pH 7.4	28
4.8.4 Drug release profile at pH 2.0	29
FUTURE PROSPECTS	30
BIBLIOGRAPHY	31

TABLE OF FIGURES:

Figure 1: Two main approaches (i.e., Top-down, and Bottom-up) that can be used for the synthesis of carbon nanodots (Hea Yeom, n.d.). Top-down approaches involve breakdown of larger carbon structures to smaller ones while Bottom-up approach involves processes like condensation and carbonization.....	5
Figure 2: Show the Drug loading and drug release of Cyt on the Hydrogel. The amide linkages formed between graphene dots and cytarabine (Cyt) are responsible for loading and holding the drug into the gel. As the pH changes, the already formed amide bonds break hence releasing the drug from the hydrogel	10
Figure 3 Pectinodesmas Cultivation at 26-28oC at given light intensity for 14 days in BBM Media. Proper aeration and light intensity is ensured to obtain a good yield of strain for the experiment.....	11
Figure 4: Algal Carbon Dots that are formed showed bright Blue Glow under UV Transilluminator which is an indication of carbon material present.....	12
Figure 5: (A) Chitosan Hydrogel without Carbon Dots (B) Chitosan Hydrogel with Carbon Dots (C) Chitosan Hydrogel with Carbon Dots (under UV Light).....	13
Figure 6 Explains the process of formation of carbon nanodots from algae as a raw material through a series of steps until the final stock solution of carbon dots is obtained (Created with BioRender.com).....	14
Figure 7 Explains the process of synthesis process of chitosan hydrogel using a starter mixture of “glycerol : acetic acid” (2:3) through a series of steps till the formation of solid translucent gel with specific properties (Created with BioRender.com).....	14
Figure 8 (A) SEM analysis of (PHM3) Carbon Nanodots at X100,000 magnification displaying average size of the carbon nanodots (18.6 nm). (B) SEM analysis of (PHM3) carbon nanodots at X30,000 times magnification.....	19
Figure 9 EDX pattern of CA (PHM3 algae) nanodots.....	20
Figure 10 FTIR analysis and surface chemistry of carbon nanodots: (A) FTIR spectra of PHM3 algal strain and (B) FTIR spectra of CA (PHM3 algae) nanodots.....	21
Figure 11 XRD analysis of CA (PHM3 algae) carbon nanodots.....	23
Figure 12 UV-Vis absorption versus wavelength graph of gold nanostars with a broad absorbance peak at 664nm.....	23

Figure 13 a) Antibacterial Activity of CAVC hydrogel against E. coli. b) Antibacterial Activity of CAC hydrogel against E. coli. c) Antibacterial Activity of chitosan hydrogel against E. coli. d) Antibacterial Activity of CNs against E. Coli	24
Figure 17 a) Antibacterial Activity of CAVC hydrogel against S. aureus. b) Antibacterial Activity of CAC hydrogel against S. aureus. c) Antibacterial Activity of chitosan hydrogel against S. aureus. d) Antibacterial Activity of CNs against S. Aureus.....	25
Figure 21 Results from swelling studies	26
Figure 22 Results from degradation studies.....	27
Figure 23 Standard curve of vancomycin	28
Figure 24 Drug release curve for vancomycin at two different pH levels.....	29

LIST OF ABBREVIATIONS:

CAVC	Vancomycin loaded carbon nanodots incorporated chitosan hydrogel
CAC	Carbon nanodots incorporated chitosan hydrogel
CNs	Carbon nanodots
nm	Nanometer
ml	Milliliter
mg	Milligram
rpm	Rate Per Minute
EDX	Energy Dispersive X-ray
FTIR	Fourier Transform Infrared
XRD	X-ray Diffraction
E. coli	Escherichia Coli
UV-VIS	Ultraviolet-Visible
IR	Infrared

ABSTRACT:

Background:

Carbon nanodots (CNDs) are nanoscale carbon-based particles known for their small size (typically less than 10 nm), excellent biocompatibility, low toxicity, and strong photoluminescence. Chitosan, a biopolymer derived from chitin, is notable for its biocompatibility, biodegradability, and ability to enhance drug solubility and permeability. In drug delivery, it is possible to use CNDs as fluorescent signals for tracking the delivery process, while chitosan serves as a versatile carrier that can encapsulate drugs, facilitate their controlled release, and enhance cellular uptake due to its mucoadhesive properties. Together, they form an effective composite for targeted drug delivery systems, combining the imaging capabilities of CNDs with the drug-carrying and release properties of chitosan, potentially improving therapeutic outcomes.

Methodology:

Algae extract was used for the synthesis of carbon nanodots using hydrothermal method where algal biomass served as carbon precursor for the synthesis carbon nanodots. The synthesized carbon dots were studied by imaging microscopy, XRD, EDS, and FTIR in addition to scanning electron microscopy and ultraviolet-visible spectroscopy. Chitosan was mixed with 2:3 solution of acetic acid and glycerol and carbon nanodots were mixed in this solution during gelation process. The resulting gel was characterised by swelling and degradation studies and drug release studies were performed using UV-Vis Spectroscopy.

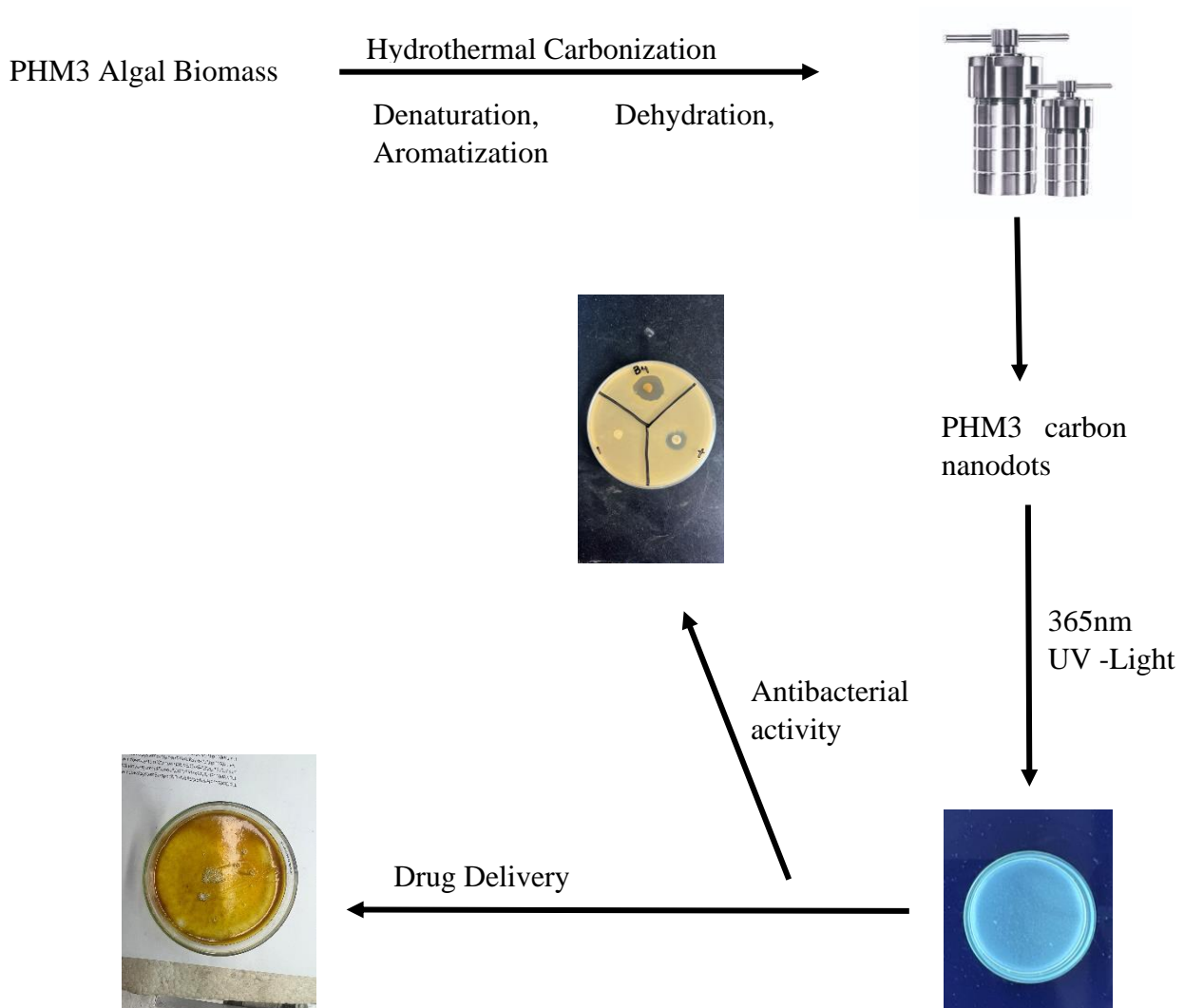
Results:

UV-Vis analysis revealed the distinct peak at 264nm attributed to Carbon nanodots whereas SEM analysis demonstrated the characteristic morphology of carbon nanodots with spherical shapes and some agglomeration. FTIR spectra of carbon nanodots confirmed presence of similar peaks when compared to algal strain with difference in intensity of peaks. Swelling studies suggested that with increase in concentration of carbon nanodots swelling properties are reduced. Degradation studies suggested that with gel with increased carbon nanodots concentration were less prone to degradation. Drug loading and releasing properties of hydrogel using Vancomycin as model drug were performed at different two different pH. Drug releasing properties were greatly enhanced in 2 pH conditions as compared to 7.4 pH.

Conclusion:

The finding suggested carbon nanodots incorporated chitosan gel could be used as possible strategy for drug delivery of drugs that have poor absorptions in gastrointestinal tract.

Graphical Abstract:



INTRODUCTION

1.1 Carbon Nanodots:

Nanoparticles, typically measuring between 1 nm and 100 nm, display markedly different properties than larger-scale materials (Simpson, 2015). Their increased surface area to volume ratio significantly enhances their optical, physical, and chemical attributes. For instance, gold nanoparticles in an aqueous solution appear red, which is a stark contrast to the gold color seen in jewelry (Simpson, 2015). Unlike the heavy metals found in semiconductor quantum dots, carbon is generally considered non-toxic. Studies on carbon dots have shown that they possess a conjugated system featuring both sp² and sp³ hybridized carbon structures and oxygen-containing functional groups (Sawant & Bamane, 2016a). These carbon dots exhibit fluorescence similar to that of semiconductor quantum dots, but with notable differences. Semiconductor quantum dots have diameters close to the Bohr exciton radius, causing a quantum confinement effect that leads to size-dependent fluorescence (Hines & Kamat, 2014). Conversely, the fluorescence of carbon dots is not strictly size-dependent. For instance, Zuo et al. (2014) synthesized carbon dots around 120 nm in size, which displayed emission spectra similar to carbon dots of approximately 10 nm. Typically, carbon dots exhibit broad emission peaks ranging from blue to near-infrared when excited with UV light (Dong et al., 2014).

Various top-down techniques have been developed to produce luminescent carbon nanodots since their first discovery. Some of the approaches include electro-oxidation, acid-assisted chemical oxidation, graphite laser ablation, and the use of lampblack or candle soot as precursors. Despite their effectiveness, these techniques often require harsh chemicals, involve complex multi-step processes, necessitate toxic reagents, and need specialized equipment (Zuo et al., 2014).

On the other hand, bottom-up methods for carbon dot synthesis are often described in the literature as being simpler, more cost-effective, and environmentally friendly. These methods typically utilize substances like glucose, glycol, sucrose, glycerol, and citric acid to produce carbon dots through hydrothermal treatment (Xiaoming Li et al., 2015), microwave-assisted techniques, and thermal decomposition. Recently, there has been a growing trend toward using natural resources for carbon dot synthesis via hydrothermal carbonization. These methods are not only simple, cost-effective, and environmentally friendly but also yield carbon dots with excellent photoluminescent properties and high quantum yield. Examples include using

materials such as orange peels, soy milk, milk, pomegranate (Kasibabu et al., 2015), and gram seeds (Das et al., 2017).

Due to their good photostability and biocompatibility, carbon dots have been utilized by various research groups for bioimaging applications (Esteves da Silva & Gonçalves, 2011). Additionally, carbon dots have been conjugated with anticancer drugs to monitor drug pathways and evaluate anticancer activity (Sachdev et al 2016). Moreover, some carbon dots have demonstrated intrinsic anticancer activity, potentially eliminating the need for drug conjugation (Hsu et al., 2013b).

With the growing interest in carbon nanomaterials, carbon nanodots (CNDs) have become a significant focus of research. CNDs show great promise for various biomedical applications, including therapy, imaging, and drug delivery. They can function as contrast agents, helping to assess biodistribution and biocompatibility prior to clinical use. Compared to other carbon nanomaterials, CNDs offer several advantages, such as enhanced biocompatibility, reduced toxicity, and environmental friendliness. Furthermore, the photophysical and chemical properties of CNDs, such as their size and shape, can be tailored to improve their biocompatibility and targeting capabilities. This adaptability enhances their selectivity and sensitivity, expanding their range of applications. Additionally, carbon nanomaterials can be engineered to innovate therapeutics and boost drug targeting efficiency (Mohd Sameer et al., 2023).

1.2 Hydrogels:

Hydrogels are polymer networks that have been cross-linked and include many hydrophilic groups or domains. The networks exhibit high hydrophobicity and adhere strongly due to the intermolecular bonds formed between the polymer chains. Hydrogels undergo expansion and assume their characteristic form when they come into contact with water. Once hydrogels reach their maximum volume, they acquire the properties of living tissues, such as a flexible and elastic texture, and exhibit little stress at the interface when in contact with water or biological fluids. Hydrated hydrogels alleviate post-implantation tissue pain due to their elastic properties. The hydrogel surface's low interfacial tension with bodily fluids reduces both protein adsorption and cell adhesion, hence minimizing the probability of adverse immunological responses.

In addition, hydrogels are well-suited for drug delivery due to a number of their properties. Polyacrylic acid (PAA), poly(2-hydroxyethyl methacrylate) (PHEMA), polyethylene glycol (PEG), and polyvinyl alcohol (PVA) are all common polymers in hydrogels, and they all have bioadhesive and mucoadhesive properties. Both the drug's solubility and its ability to cross blood-tissue barriers are enhanced by these features. The hydrogel's sticky quality comes from the fact that its functional groups form inter-chain bridges with mucus glycoproteins. This enables specific binding to organs such the vagina, nose, and colon.

Hydrogels exhibit variable dimensions, ranging from nanometers to centimeters in width, and possess notable deformability, enabling them to conform to the contours of their surroundings. Furthermore, owing to their physiochemical resemblance to the native extracellular matrix—both in composition (e.g., glycosaminoglycans) and mechanical properties—hydrogels can fulfill dual roles. They can serve as supportive scaffolds for cells during tissue regeneration while facilitating the delivery of therapeutic agents (Narayan Bhattarai et al., 2010).

Highly hydrated, hydrogels are crafted from cross-linked polymers, facilitating sustained, localized delivery of diverse therapeutic agents. The utilization of chitosan, a natural polymer, in hydrogel formulations has garnered significant attention due to its biocompatibility, low toxicity, and biodegradability. The advancement of chitosan-based hydrogels has paved the way for novel drug delivery systems capable of releasing payloads in response to various environmental cues. Additionally, thermosensitive hydrogel variants have emerged, allowing for in situ formation of chitosan hydrogels, eliminating the need for surgical implantation. The development of these intelligent drug delivery platforms necessitates a profound understanding of the chemical and physical attributes of chitosan-based hydrogels, as well as the characteristics of the therapeutics being delivered (Narayan Bhattarai et al., 2010).

1.3 Drug Delivery System:

Drug delivery systems have evolved significantly, transitioning from conventional methods like pills and injections to advanced systems designed for targeted and controlled release of therapeutics. Traditional approaches often suffer from limitations such as poor bioavailability, frequent dosing requirements, and systemic side effects. To overcome these challenges, modern drug delivery technologies, including nanoparticles, liposomes, and biodegradable polymers, have been developed. These systems enhance the precision and efficiency of drug administration, ensuring that medications reach specific sites within the body and release their

active ingredients at a controlled rate. This approach minimizes side effects and improves therapeutic outcomes, particularly in treating chronic diseases and cancers (Xiaoxiao Cheng et al 2023).

Vancomycin, a glycopeptide antibiotic, is often used to treat severe bacterial infections caused by Gram-positive organisms, including methicillin-resistant *Staphylococcus aureus* (MRSA). It is a crucial medicine in the fight against antibiotic-resistant infections since it inhibits bacterial cell wall synthesis. However, vancomycin's effectiveness can be limited by poor oral bioavailability and the need for intravenous administration. This has spurred research into advanced delivery systems, such as encapsulating vancomycin in nanoparticles or liposomes, to enhance its stability, target infection sites more effectively, and reduce toxicity. These innovations aim to improve patient outcomes by optimizing drug release and minimizing adverse effects (Xiaoxiao Cheng et al 2023).

The researchers used *Pectinodesmus* sp., a species of microalgae found in freshwater, for their study. Algae are capable of producing several nutraceuticals, including lipids, minerals, vitamins, proteins, and polysaccharides. Baky and El-Baroty (2013) reported that algae contain bioactive compounds with notable properties that might potentially be used in the treatment of cancer, inflammation, oxidative stress, and other age-related diseases. The work used a green hydrothermal carbonization method to generate carbon nanodots (CA-PHM3) from the algae strain *Pectinodesmus* sp.

A comparative study of Carbon nano dots and Chitosan hydrogel properties was carried out to achieve the following objectives:

1. To synthesis carbon nanodots through hydrothermal process
2. To Incorporate carbon nanodots into chitosan matrix
3. To investigate drug loading and releasing properties of chitosan gel

LITERATURE REVIEW

2.1 Carbon nanodots Discovery:

Carbon nanodots were discovered accidentally during the process of electrophoretic distillation of carbon nanotubes (SWCNTs) by (Xu et al., 2004a). Besides single walled carbon nanotubes, some fluorescent particles from crude were isolated as an impurity. These fractions show yellow, orange, and green-blue light (500-600nm) when exposed to 365nm. Those showing orange color had a size of 18nm and when analyzed via FTIR revealed the existence of multiple carboxylic groups.

2.2 Synthesis of carbon:

There are two main approaches that can be used for synthesis of carbon nanodots:

- Top-Down Approach: involves oxidation of larger graphite particles into smaller carbon nano particles using powerful techniques.
- Bottom-Up Approach: involves the use of methods like condensation and carbonization upon different carbon sources.

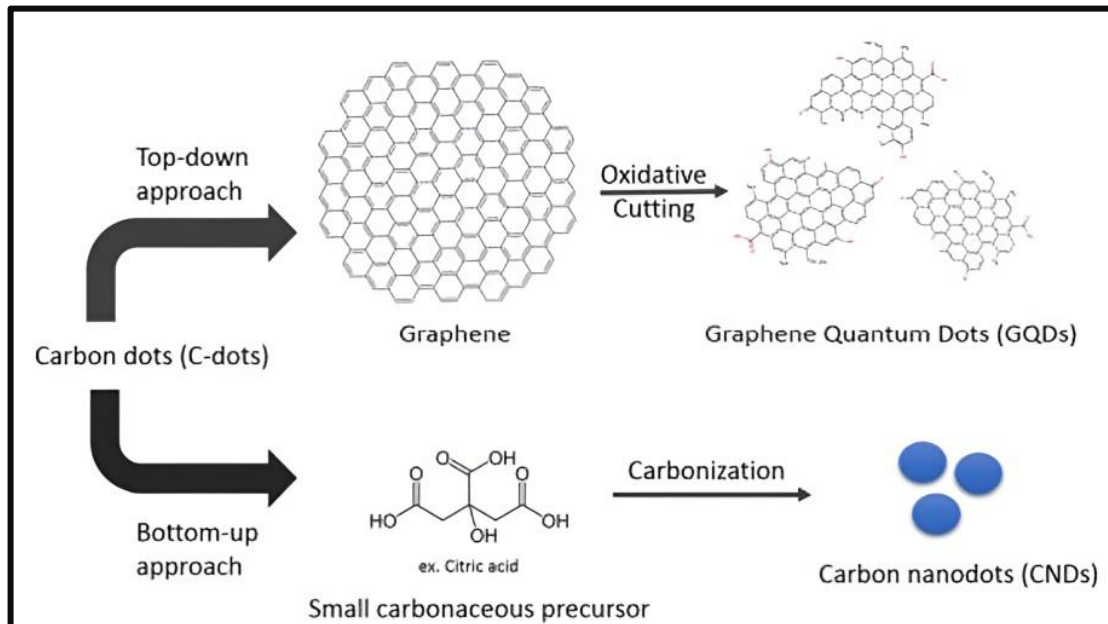


Figure 1: Two main approaches (i.e., Top-down, and Bottom-up) that can be used for the synthesis of carbon nanodots (Hea Yeom, n.d.). Top-down approaches involve breakdown of larger carbon structures to smaller ones while Bottom-up approach involves processes like condensation and carbonization.

2.2.1 Top-Down Approaches for Synthesis of Carbon Nanodots:

Top-down approaches for synthesizing carbon nanodots include following:

2.2.1.1 Laser Ablation:

Laser ablation involves synthesizing carbon dots from bulky materials of carbon (S.-L. Hu et al., 2009) reported such a technique for synthesis, by exposing a solution of carbon material in an organic solvent to laser radiation. During this, the photoluminescent origin was attributed to the functional groups on the surface of carbon nanodots. They also proposed that the fluorescence emission can also be changed by doing some modifications on the surface functional groups that can be performed by using different types of organic solvents. Another approach for luminescent dots synthesis was proposed by (Xiangyou Li et al., 2011) in which nanocarbon was used as a solvent. The process starts with dissolution of 0.02g of nanocarbon 50ml of solvent i.e., acetone, ethanol or water. This mixture was then ultrasonicated. Afterwards a 4ml of suspension was taken and then subjected to laser irradiation. After irradiation the solution was centrifuged in order to separate supernatant containing fluorescent carbon dots. The surface chemistry of carbon nanodots highly depends on the organic solvent in which the carbon material was prepared.

2.2.1.2 Electrochemical Carbonization:

Electrochemical carbonization serves as another important top-down technique to synthesize carbon dots from bulky carbon material. Literature provides some information regarding the synthesizing carbon dots using this approach for example, (J. Deng et al., 2014) describes the synthesis of carbon dots through the process of electrochemical carbonization alcohols having small molecular weight. The study involved use of two Pt (platinum) sheets as auxiliary and working electrode while another calomel electrode was freely adjusted and used as a reference. In the process different alcohols were converted into carbon dots. The carbon dots synthesized by the mentioned routes had an increased degree of graphitization along with an increasing applied potential.

2.2.1.3 Exfoliation of Carbon Soot:

Another top-down technique for preparation of carbon dots is incomplete combustion of candle, lamps, and plants like, (H. Liu, Ye, & Mao, 2007) reported the synthesis of carbon dots from candle soot, which had a high stability that lasted for several months. The surface of these carbon dots had carboxylic acid groups which allowed bonding with biomacromolecules via hydrogen bonding and other electrostatic interactions. Wei et al., 2013 proposed the method

for synthesizing carbon dots from paper ash, by a simple and environmentally friendly procedure. Paper ash was dispersed in deionized water followed by the process of filtration. After that centrifugation was performed in order to separate the supernatant which was further dialyzed against pure distilled water for separating any impurities or any inorganic ions. A transparent solution was obtained at this point which contained carbon dots. Carbon dots prepared from this paper ash had an average diameter of 3nm.

2.2.2 Bottom-up Approaches for Synthesis of Carbon nanodots:

Top-down approaches are powerful yet very common. However, they do have some disadvantages like the use of expensive reagents and complicated instrumentation in the majority of the cases. Bottom-up approaches seem much more attractive because of their low cost and low temperature while requiring less instrumental setup.

2.3.2.1 Pyrolysis:

Pyrolysis is a very simple yet a promising method for preparation of carbon dots. Wang et al., 2010 used the same method in preparing oil and water-soluble carbon dots by simply changing the reaction solvent during pyrolysis. In a study lead by (R. Liu et al., 2013) carbon dots were prepared using poly-ethylene glycol (PEG) in one step by sodium hydroxide-assisted reflux treatment. The carbon dots blue luminescent was so strong to be visible by naked eye. Carbon dots had a spherical shape with an average diameter of 5nm.

2.3.2.2 Microwave Assisted Approach:

This approach offers an efficient energy but an intensive microwave treatment which greatly reduces the reaction time for example, (Chowdhury, Gogoi, & Majumdar, 2012) synthesized carbon dots from chitosan gel using this process. The dimensions of these carbon dots ranged from 0.6-8.7nm. The photoluminescent spectra showed an excitation dependent emission behavior. Mitra et al., 2012 used polyoxyethylene-polyoxypropylene-polyoxyethylene (PEO-PPO-PEO) block co-polymer pluronic F-68 (PF-68) and o-phosphoric acid to prepare carbon nanodots by microwave aided process within just a few minutes. The maximum PL intensity for these carbon nanodots was obtained with an excitation wavelength of 380nm. Its smission spectra showed a bathochromic shift with a decreasing intensity while an increase in excitation energy. The carbon particles obtained had a spherical morphology with size range of 5nm-20nm.

2.3.2.3 Hydrothermal Method:

The hydrothermal method offers a greater advantage as a variety of carbon sources can be used as a precursor and is a greener process for synthesis of carbon nanodots can be achieved. In procedure a carbon source (dried organic material form plat usually) is transferred to a Teflon lined stainless steel autoclave and heated at a range in between 180-240°C for hours. During the high heat and pressure treatment the solution changes its color from colorless to brown which indicates that the reaction is completed. This method avoids multistep passivation, complex instrumentation and expensive reagents. Zhu et al., 2012 described the hydrothermal treatment of soy milk for synthesizing carbon dots which had a brilliant water solubility and also displayed a blue color under UV-lamp (365nm). Similarly, (Sahu, Behera, Maiti, & Mohapatra, 2012) used hydrothermal carbonization on orange juice for synthesis of carbon dots at a low temperature (i.e.,120°C). In a lesser time (i.e., 150 min) green, fluorescent carbon dots were obtained with spherical morphology that have an average size that ranged from 1.5 to 4.5nm. Fluorescence producing carbon nanodots had also been synthesized via hydrothermal treatment of ethylenediamine and citric acid by (S. Zhu et al., 2013a). Carbon dots formed were amorphous (i.e., without any lattices) but had a high quantum yield.

2.2 Carbon dots incorporation into Chitosan Hydrogel:

In the work by Konwar, A., Gogoi, N., Majumdar, G., et al. (2015), chitosan hydrogels were incorporated with carbon nanodots made by hydrothermal carbonization of a green source i.e., Tea. The chitosan's positive charge and the carbon nanoparticles' negative charge interact electrostatically. As a result, a stable and strong nanocomposite hydrogel of chitosan and carbon dots was formed. Subsequently, thermogravimetric analysis, ultraviolet-visible spectroscopy, scanning electron microscopy, XRD, FTIR, and contact angle analysis were used to describe this hydrogel. The gel outperformed chitosan hydrogel film in terms of mechanical, thermal, swelling, and UV-visible blocking qualities, as well as being a soft material with robust characteristics. A higher contact angle value for the hydrogels containing chitosan and carbon dots suggests that they are hydrophobic, or resistant to water.

2.3 Drug Delivery properties of CQD:

Researchers Konwar et al. found that aloe vera leaves had bright carbon dots (2015). The formed carbon quantum dots were structurally analyzed using methods such as fluorescence

spectroscopy, X-ray photoelectron spectroscopy (XPS), surface polarity, hydrodynamic diameter, Fourier transform infrared spectroscopy (FTIR), Raman, and high resolution transmission electron microscopy (HRTEM). Their high water dispersibility and lack of cytotoxicity inspired their incorporation into a calcium alginate hydrogel film for the purpose of regulating the gastrointestinal (GI) tract delivery of the glycopeptide antibiotic vancomycin. Adding carbon dots increased the drug loading capacity from 38% to 89%. When β -cyclodextrin (β -CD) was loaded with Vancomycin, the drug loading capacity of the latter was increased to 96% with the addition of carbon dots. At a pH of 1.5, which is comparable to the pH of the stomach (1-2), vancomycin was released most efficiently. Nevertheless, the release was decreased to 56% during the subsequent 120 hours when β -cyclodextrin (β -CD) was added. Because of its high loading capacity and slow release, this feature may find use in drug delivery systems.

Graphene Quantum dots were prepared using citric acid (Sheng, Y., Dai, W., Gao, J., Li, H., Tan, W., Wang, J., Deng, L., Kong, Y. (2020)). These graphene dots were used for loading cytarabine (hydrophilic). The drug was wrapped in chitosan hydrogel to ensure encapsulation of loaded cytarabine (Cyt). By the use of chitosan hydrogel, the stability of graphene dots increased significantly which can be due to inhibited agglomeration of Graphene dots by the Chitosan hydrogels. Also, the release of Cyt from the developed carrier was also effectively relieved by the chitosan coating. As amide reaction was responsible for incorporation of Cyt into Graphene dots, the hydrolysis of amide linkages was responsible for pH sensitive delivery of cytarabine (Cyt).

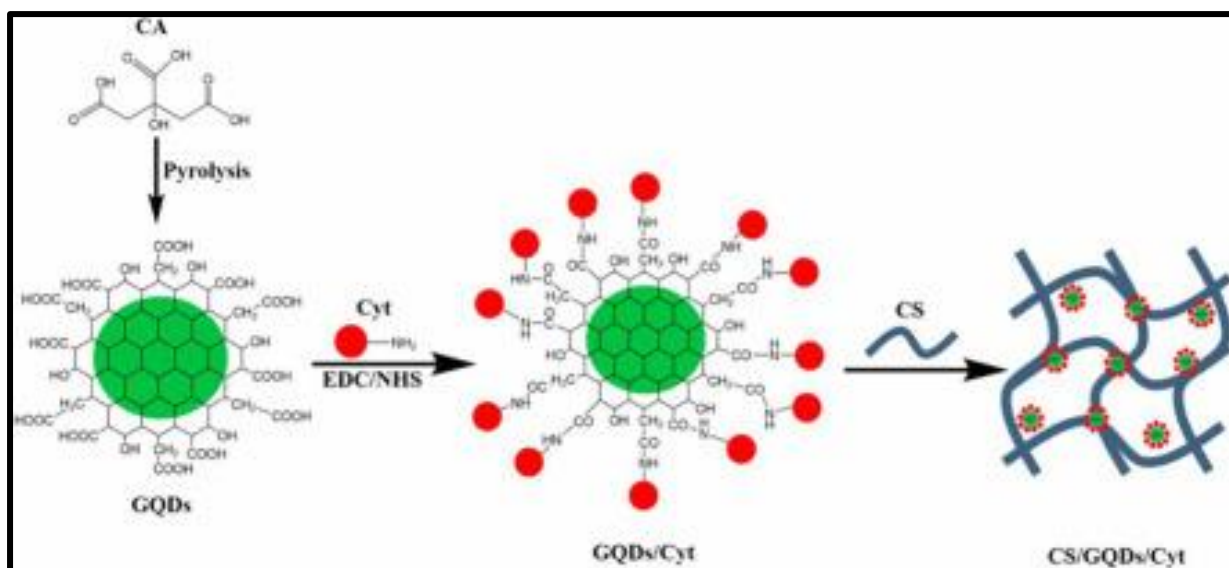


Figure 2: Show the Drug loading and drug release of Cyt on the Hydrogel. The amide linkages formed between graphene dots and cytarabine (Cyt) are responsible for loading and holding the drug into the gel. As the pH changes, the already formed amide bonds break hence releasing the drug from the hydrogel

MATERIALS AND METHODS

3.1 Hydrothermal Synthesis of Carbon nanodots:

Cultivating of microalgae *Pectinodesmus* alga strain LC159307 previously identified and collected by (Khalid et al., 2017) and then was cultured in liquid BBM Bold basal media. The media was poured in the Flasks/Bottles that contained microalgal inoculum. A fluorescent, white tube-light with $100 \mu\text{mol}$ of photons $\text{m}^{-2}\text{s}^{-1}$ was used with a 25-hour light cycle along with ensuring continuous aeration by including air pumps in the setup. The culture was maintained at temperature at 26-28 °C for 14 days. Algae was harvested and transferred into petri dishes. The algae were dried using a drying oven set to 60°C temperature. The dried algae were scratched microalgae on petri plate with scapula Grinding microalgae with motor and pestle into dried fine powder like material microalgae.

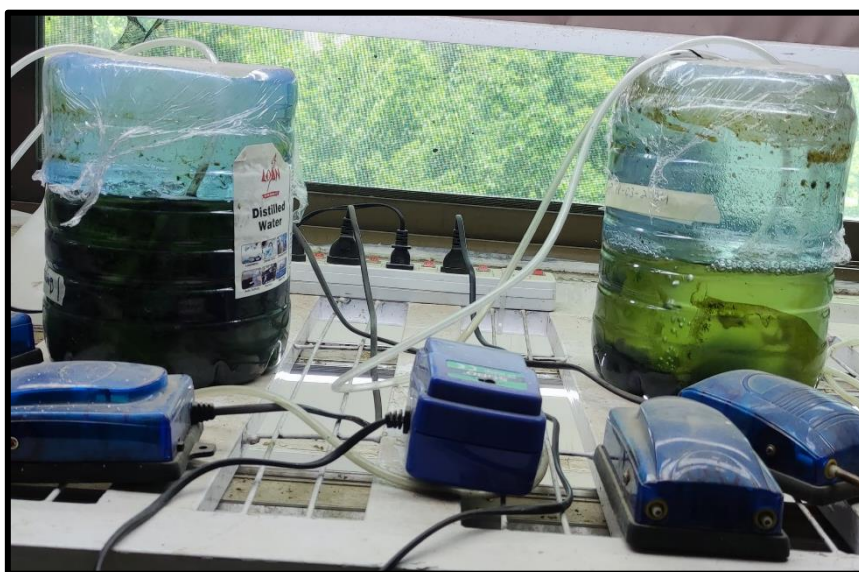


Figure 3 Pectinodesmus Cultivation at 26-28oC at given light intensity for 14 days in BBM Media. Proper aeration and light intensity is ensured to obtain a good yield of strain for the experiment.

1g from powdered dry algal mass was then dissolved in 50ml of distilled water at a temperature ranging from 50 to 60°C along with continuous stirring for about 10 to 15 minutes on a magnetic stirrer. The greenish solution obtained was then transferred into Teflon autoclave chamber and sealed properly to avoid leakage, autoclave was then placed in the heating oven that was pre-heated at 200°C. The reaction was allowed to be completed in 3 hr. Once the

reaction is completed, the autoclave is left to cool at room temperature. The resulting dark brownish solution obtained was then undergone through centrifugation at 16000rpm for 30min to eliminate any larger impurities that might have formed during the carbonization process. After centrifugation was completed, the supernatant was collected, and using syringe filter (0.22 μ m) any further large size particles were removed resulting in a dark brown solution obtained that contained Carbon nanodots (CN).

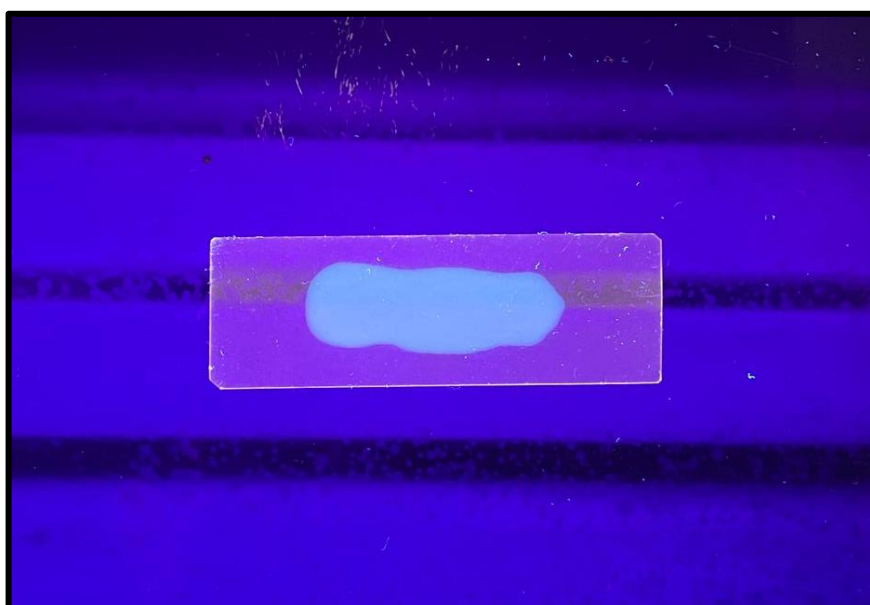


Figure 4: Algal Carbon Dots that are formed showed bright Blue Glow under UV Transilluminator which is an indication of carbon material present.

3.2 Chitosan Hydrogel Formation:

A straightforward procedure was used to create the chitosan hydrogel film (Konwar et al., 2015):

1. A solution was made by mixing 0.1 M acetic acid with stock glycerol, which is two parts glycerol and three parts acetic acid (2:3).
2. At room temperature for 2 hours, a magnetic stirrer was used to mix 0.1 g of chitosan with 10 ml of the solution that had been made earlier. This made sure that the powdered chitosan dissolved completely in the specified liquid.
3. To neutralize the aforementioned combination, a 5 N sodium hydroxide (NaOH) solution was added dropwise while stirring continuously. This not only neutralizes the acid, but it also

distributes the NaOH properly inside the preceding (if added earlier, it would induce foam formation).

4. An opaque, milky, sticky gel was produced at the neutralization point. To get rid of any unreacted monomer, the produced gel was rinsed with Millipore water many times.

5. A hydrogel film containing nanocomposite chitosan carbon dots was produced using the same method as hydrogels containing chitosan. In this case, in addition to the chitosan and "acetic acid: glycerol" combination, a weight percentage of 30% algal CDs was also added. Our preferred option is the fact that acetic acid is soluble in chitosan was considered while choosing carbon dots. After that, the solutions were left to mix at room temperature for two hours using a magnetic stirrer. To prevent foaming, carbon dots were added during the final half an hour of stirring. After that, the gel is neutralized with 5 N NaOH.

6. The hydrogel is washed many times with Millipore water to remove any unreacted monomers. Then, the gels are cast on glass plates and let to cure at room temperature for 24 hours.

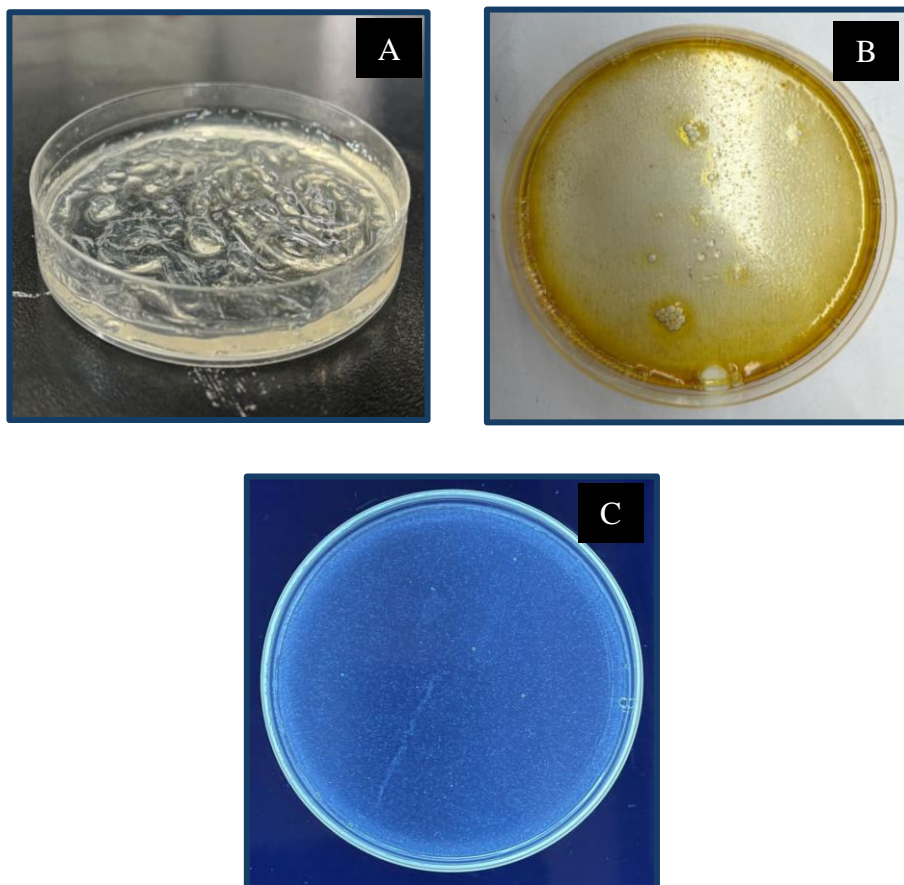


Figure 5: (A) Chitosan Hydrogel without Carbon Dots (B) Chitosan Hydrogel with Carbon Dots (C) Chitosan Hydrogel with Carbon Dots (under UV Light)

3.3 Graphical Methodology:

3.3.1 Synthesis of Carbon Nanodots:

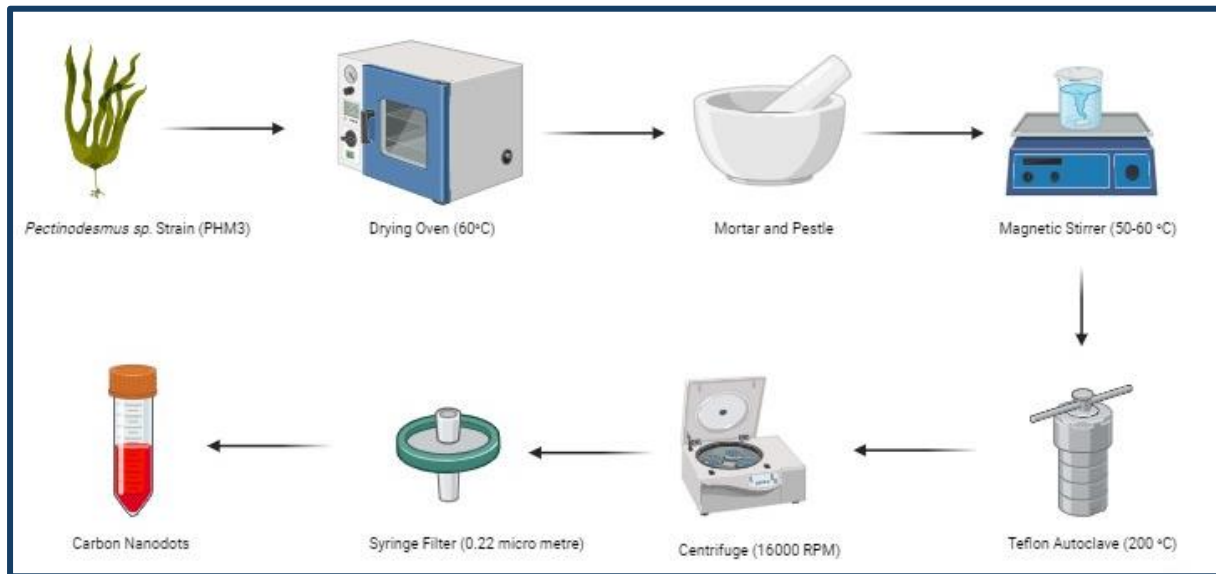


Figure 6 Explains the process of formation of carbon nanodots from algae as a raw material through a series of steps until the final stock solution of carbon dots is obtained (Created with BioRender.com)

3.3.2 Formation of Chitosan Hydrogel:

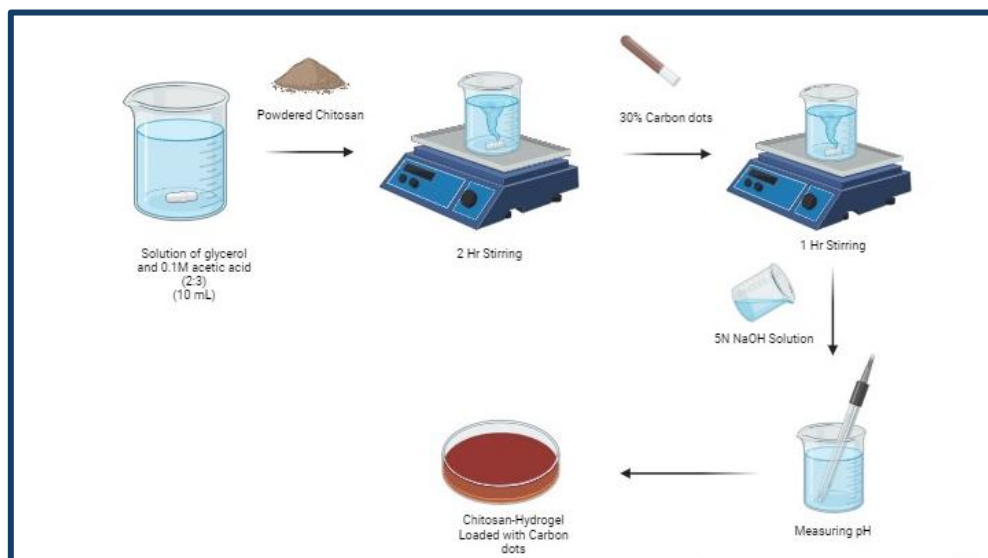


Figure 7 Explains the process of synthesis process of chitosan hydrogel using a starter mixture of “glycerol : acetic acid” (2:3) through a series of steps till the formation of solid translucent gel with specific properties (Created with BioRender.com)

3.4 Characterization of Carbon Nanodots:

3.4.1 Scanning electron microscopy (SEM):

Carbon nanodots morphology was analyzed using SEM (Joel JSM-6490LA).

3.4.1.1 Sample Preparation:

For SEM analysis, a drop of carbon nanodots of PHM3 algae was diluted up to tenfold in water. It was then sonicated in an Eppendorf tube using an ultrasonicator (Cole-Parmer) for 20 minutes to disperse the particles evenly and break up any agglomerates. Subsequently, a drop of the dispersion was placed onto a 1cm×1cm slide using a micropipette and dried in a drying oven at 50°C for one hour. Following this, the sample underwent gold coating using a sputter coater to ensure surface conductivity. The coated samples were then mounted onto stubs using conductive tape and subjected to scanning electron microscopy (SEM) at 20eV, with varying magnifications of 50,000X and 100,000X.

3.4.2 Energy Dispersive X-ray Spectroscopy (EDX or EDS):

EDX analysis was conducted concurrently with SEM to ascertain the elemental composition of carbon nanodots.

3.4.2.1 Sample Preparation:

To prepare the sample, a droplet of carbon nanodots of PHM3 was dried on a glass slide in an oven for 10-15 minutes. EDS analysis of the sample was conducted at 20eV with a probe current of 1mA to detect the presence of carbon nanodots.

3.4.3 Fourier Transform Infrared Spectroscopy (FTIR):

The functional groups on the surface of carbon nanodots were assessed using the Perkin-Elmer Spectrum-100 spectrometer.

3.4.3.1 Sample Preparation:

FTIR measurements were performed with the Perkin-Elmer Spectrum-100 spectrometer, covering a wavelength range from 450 to 4000 cm^{-1} . Two samples, namely carbon nanodots of PHM3 and the PHM3 algal strain, were analyzed. Due to its hygroscopic nature, KBr was utilized for sample preparation. For both of carbon nanodots of PHM3 and the PHM3 algal strain, concentrated solutions were first centrifuged to obtain pellets. These pellets were then used to create KBr pellets using a hydraulic press. The pellets were placed in the IR chamber where infrared rays were directed onto them.

3.4.4 X-ray Diffraction Spectroscopy:

X-ray diffraction (XRD) is acknowledged as a highly effective technique for identifying the crystalline phases within materials.

3.4.4.1 Sample Preparation:

A lyophilized sample of carbon nanodots was applied onto a glass microscope slide, which was then inserted into the XRD chamber.

3.4.5 UV-Vis Analysis:

Utilizing a UV-VIS spectrophotometer, absorption spectra graphs were generated for the solution containing CA (PHM3 algae) nanodots. The absorbance spectrum of the carbon nanodots of PHM3 was examined across wavelengths ranging from 200 to 900 nm.

3.4.5.1 Sample Preparation:

The solution containing CA (PHM3 algae) nanodots was subjected to ten minutes of sonication in an ultrasonic bath to prepare the sample. Subsequently, the liquid solution of CA (PHM3 algae) nanodots was transferred into cuvettes and dispatched to the laboratory to obtain the absorption spectrum of the nanodots.

3.4.5 Antibacterial Assay:

Antibacterial assays were conducted on four samples: chitosan hydrogel, CA (PHM3 algae) nanodots, chitosan hydrogel with vancomycin (CAVC), and vancomycin alone, against both the strains of bacteria, i.e., *S. aureus* and *E. coli*.

3.4.5.1 Bacterial Growth:

The *E. coli* and *S. aureus* bacteria, obtained from Ms. Hina at the UG Industrial lab, ASAB, were revived from preserved glycerol stocks. The revival process took place in a clean, sterile environment provided by a class III laminar flow cabinet. All equipment involved in handling bacterial cultures underwent sterilization for 120 minutes in an autoclave.

3.4.5.2 Growth of *S. aureus* and *E. coli*:

Bacterial cultures of *E. coli* and *S. aureus* were initially revived on LB agar (Luria-Bertani). LB agar was prepared by dissolving 14 grams of nutrient agar in 500 milliliters of distilled water using a 100-milliliter Erlenmeyer flask. The nutrient agar was then heated in an autoclave at 15 psi pressure for 120 minutes. To promote bacterial growth on solid media, LB agar was dispensed into sterile petri dishes inside a laminar flow cabinet and allowed to solidify at room

temperature. Meanwhile, the glycerol stocks of *E. coli* and *S. aureus* were kept on ice. A streaking loop was sterilized in the Bunsen burner flame, and bacteria were streaked from frozen cultures onto the petri plates in four quadrants. The streaked plates were subsequently incubated at 37°C overnight to allow for growth.

3.4.5.3 Disk Diffusion Method:

The antibacterial efficacy of chitosan hydrogel, CA (PHM3 algae) nanodots, CAVC hydrogel, and vancomycin was assessed using the disc diffusion method. A sterile cotton swab was immersed in LB culture media and used to inoculate agar plates by streaking in a back-and-forth motion. The plate was then rotated 45 degrees, and this process was repeated four times. Discs approximately 6 mm in diameter were prepared from Whatman filter paper Grade 4 and sterilized by autoclaving. These discs were then soaked overnight in a solution of CA (PHM3 algae) nanodots. A single disc was placed on the agar inoculated with the bacterium using a sterile syringe. Additionally, 10 mm pieces of chitosan hydrogel and CAVC hydrogel were cut and placed on the agar, acting as negative and positive controls, respectively. The plates were incubated overnight at 37°C, and the diameters of the inhibition zones at various concentrations were measured. Each experiment was performed in duplicate, with deionized water as the negative control and ampicillin as the positive control.

3.4.6 Swelling and Degradation Studies:

In vitro swelling and degradation tests were performed at a physiological temperature of 37°C and a pH of 7. Initially, samples were precisely weighed (W_i) and then immersed in 20 mL of water. To measure the swelling ratio, samples were periodically taken out, blotted with filter paper to remove excess surface water, and reweighed (W_t). Degradation was evaluated by drying the samples in an oven at 50°C for two days, after which they were reweighed ($W_t(d)$). The swelling ratio and degradation were calculated using the following equations:

$$\text{Swelling ratio} = \frac{W_t - W_i(d)}{W_i}$$

$$\text{Degradation} = \frac{W_t - W_i}{W_i} \times 100\%$$

3.4.7 Drug delivery studies:

3.4.7.1 Drug Loading (%):

The PHM3 nanodots were investigated to check their release behaviour in-vitro. through calculating the absorbance values using a UV-visible spectrophotometer, with vancomycin as

the model drug. The drug loading capacity of the hydrogel was determined using the formula by taking average of three values from this formula:

$$\text{Drug loading (\%)} = \frac{W_{ald} - W_{bld}}{W_{bld}} \times 100\%$$

where W_{ald} and W_{bld} denote the weight of the hydrogels after and before loading with the vancomycin antibiotic, respectively. Subsequently, the dried hydrogels were immersed in 20 mL of double-distilled water to **analyse** their release profiles.

3.4.7.2 In-vitro Drug Release Studies:

After that, 30 mL of double-distilled water was added to the dried hydrogels so that we could examine their release patterns. Two different pH values, 2 and 7.4, were used to test the hydrogels' pH-responsive characteristics. To keep the volume constant for the UV-visible spectroscopic observations, 3 mL aliquots were taken from the release media at regular intervals and put back into the original medium after each experiment. Using UV-visible absorption measurements at a wavelength of 281 nm for each sample, the cumulative percentage of vancomycin released from the CAVC hydrogel was calculated.

3.4.7.3 Standard calibration curve for drug release profile:

A standard curve for vancomycin ranging from 5 to 0.25 mg/ml was established. To generate the standard curve, a 1 mg/ml stock solution of vancomycin was prepared in a water solution and serially diluted to obtain known concentrations. Each sample was then analyzed in a UV spectrophotometer at 281 nm. Three measurements were taken, and average value was calculated. A standard curve was generated. After this, the drug release % was calculated by the use of this equation:

$$\text{Drug Release Percentage} = \frac{\text{Concentration of vancomycin in sample aliquot}}{\text{Concentration of vancomycin initially added}} \times 100$$

RESULTS:

4.1 SEM Analysis of (PHM3) Carbon Nanodots:

Nanodots Scanning electron microscope is a perfect technique to analyze morphology of carbon nanodots. SEM image of (PHM3) carbon nanodots is shown in figure.

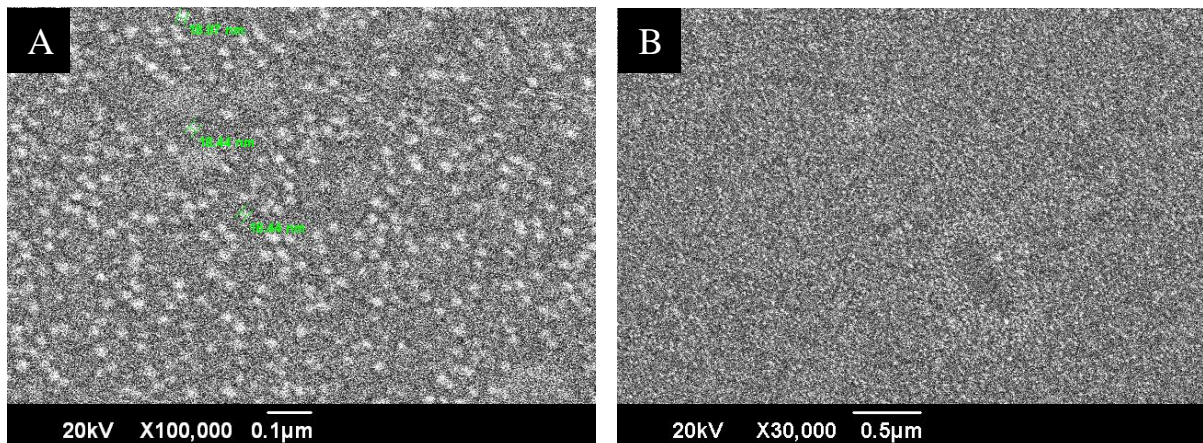


Figure 8 (A) SEM analysis of (PHM3) Carbon Nanodots at X100,000 magnification displaying average size of the carbon nanodots (18.6 nm). (B) SEM analysis of (PHM3) carbon nanodots at X30,000 times magnification.

The SEM images showed that the sizes of all the carbon nanodots are in nano-range. It also displays the spherical morphology of carbon nanodots.

4.2 EDX Results of (PHM3) Carbon Nanodots:

Using EDS, an elemental study of carbon nanodots was carried out to determine their elemental makeup. Figure displays the EDX pattern of the nanodots of (PHM3) carbon nanodots.

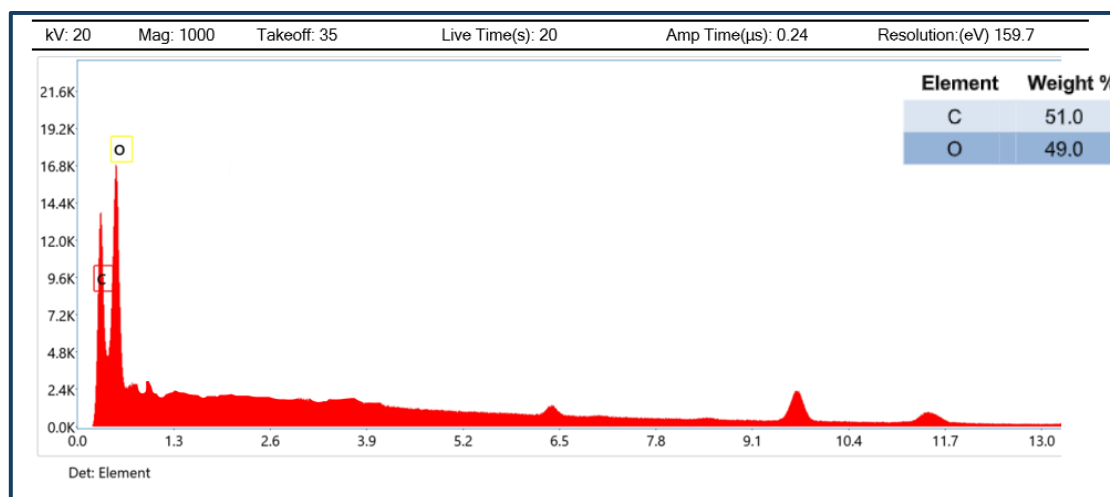


Figure 9 EDX pattern of CA (PHM3 algae) nanodots

The carbon content of (PHM3) carbon nanodots is high, with a weight percentage of 51.0%, while the oxygen content is 49.0%, according to the EDX spectrum. This suggests that the surface of the algae has been more heavily oxidized. Moreover, no contaminants were discovered.

4.3 FTIR Analysis of (PHM3) Carbon Nanodots:

FTIR analysis was used to examine the nanodots. The functional group modifications that occur during the manufacture of (PHM3) carbon nanodots are shown in figure.

Concerning the algal strain depicted in Figure 4.7.5.1 (A), the peaks observed at 3421 cm^{-1} and 2855 cm^{-1} predominantly arise from the CH_2 antisymmetric stretching vibrations of methyl groups, primarily found in lipids. Additionally, these peaks are attributed to the stretching vibrations of N-H in proteins and O-H in carbohydrates, as documented by Bankoti et al. (2017). Carbonyl groups $\nu(\text{C}=\text{O})$ are linked to the peak at 1748 cm^{-1} . A bond in an amide is linked to the peak at wavenumber 1657 cm^{-1} , whereas an amine III C-N bond is linked to the peak at wavenumber 1465 cm^{-1} (Z. Yang et al., 2014). Similarly, functional groupings of carbohydrates are linked to tiny peaks between 1200 and 726 cm^{-1} .

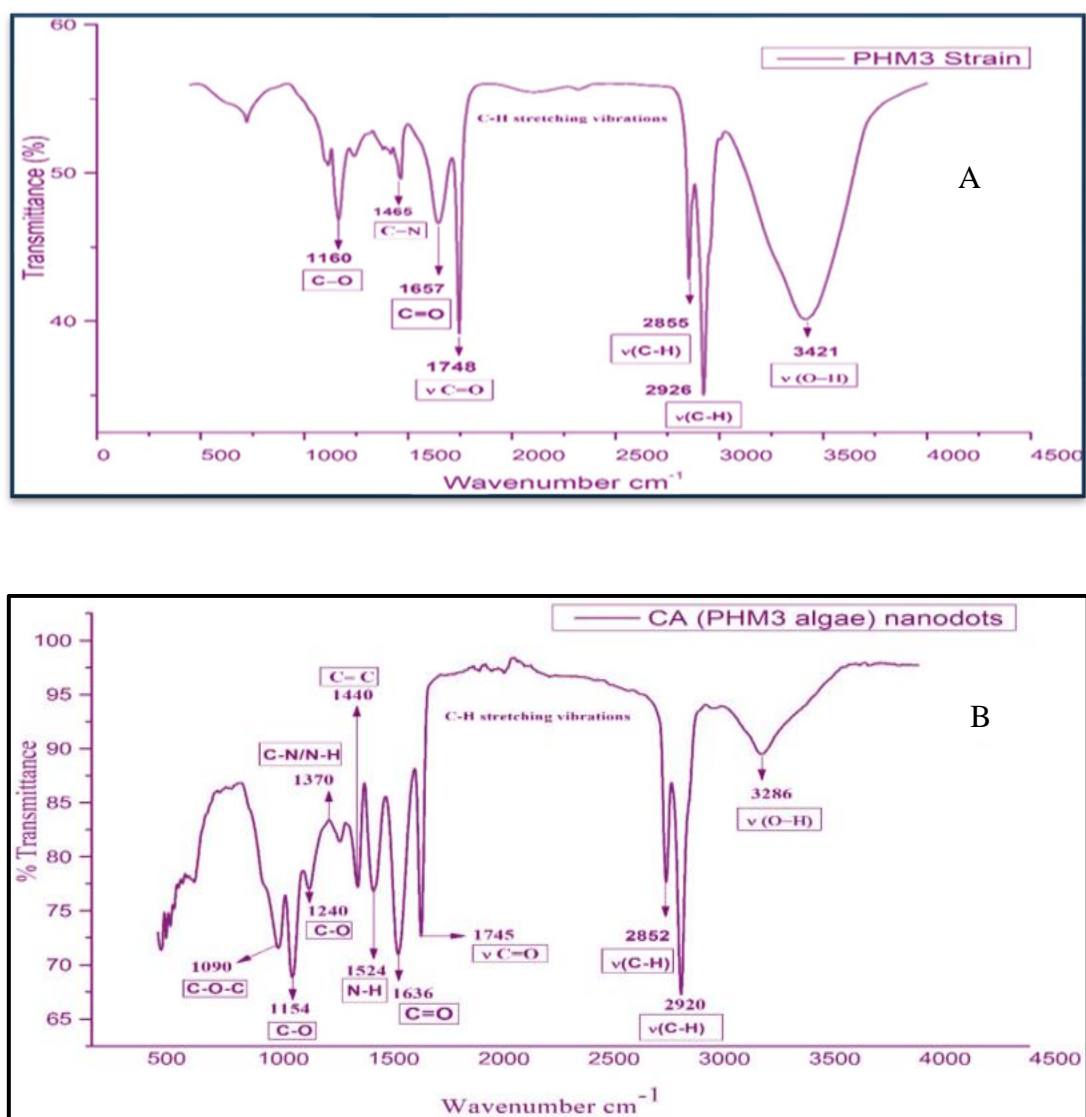


Figure 10 FTIR analysis and surface chemistry of carbon nanodots: (A) FTIR spectra of PHM3 algal strain and (B) FTIR spectra of CA (PHM3 algae) nanodots.

The FTIR spectra of the algal strain incorporated into CA (PHM3 algae) nanodots displayed significant variations in peak positions and intensities compared to the original. For instance, in Figure 4.7.5.1 (B), the peak observed at 3286 cm^{-1} exhibited a notably reduced intensity, indicating substantial consumption of O-H and N-H groups during the hydrothermal process. A similar trend was observed for peaks at 2920 cm^{-1} and 2852 cm^{-1} , suggesting a breakdown of C-H bonds. Moreover, the intensity of carbonyl groups $\nu(\text{C}=\text{O})$ in CA (PHM3 algae) nanodots was diminished, suggesting the cleavage of $-\text{COOH}$ bonds in the hydrothermal process.

The stretching frequency of aromatic carbonyl groups' C=O was connected with the peak at 1636 cm^{-1} , which was the location of the CA (PHM3 algae) nanodots' peak, but the aromatic C=C bonds' peak was at 1440 cm^{-1} . In addition, CA (PHM3 algae) nanodots showed the appearance of a new peak at 1524 cm^{-1} , which was associated with the vibration and deformation band of N-H and suggested the existence of functional groups containing amino acids.

In addition, the dehydration process between carboxyl and amino groups was indicated by the peak at 1370 cm^{-1} , which was connected with both C-N and N-H groups. This bond was thought to be an amide bond. Increased oxidation was shown by the more prominent C-O bands in CA (PHM3 algae) nanodots. The FTIR analysis showed that several parts of the PHM3 algae strain, notably carbs and proteins, were involved in the CA nanodot production.

4.4 XRD Analysis of CA (PHM3 algae) nanodots:

X-ray crystallography was used to investigate the crystal structures of the nanodots. The XRD pattern of CA (PHM3 algae) nanodots reveals the 002 diffraction patterns of graphitic carbon. These patterns indicate an interlayer spacing distance of $d_{002} = 0.36\text{ nm}$, which is slightly larger than the interlayer spacing distance of graphite (0.34 nm). Additionally, a broad peak is seen at $2\theta = 22^\circ$. The broader peak seen is indicative of poor crystallization because to the higher interlayer gap. In addition, the graphene-like structures inside the CA (PHM3 algae) nanodots exhibit in-plane diffraction, resulting in a distinct and precise peak at an angle of 44° . This peak corresponds to the presence of 101 planes.

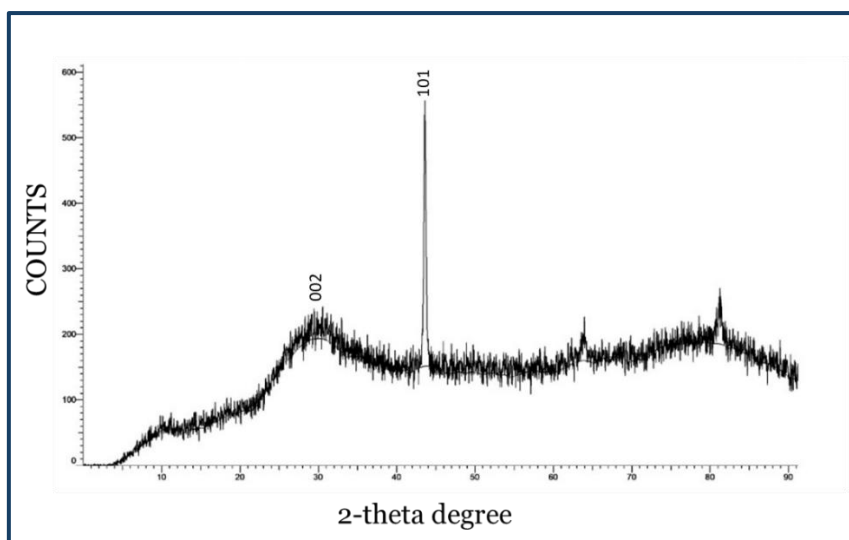


Figure 11 XRD analysis of CA (PHM3 algae) carbon nanodots.

4.5 UV- Vis Spectrophotometry of PHM3 algae carbon nanodots:

The UV-Vis absorption vs wavelength graph of PHM3 algae carbon nanodots is displayed in Figure 4. It has a broad peak in the 200–400 nm range, with the greatest absorbance recorded at 264 nm wavelength.

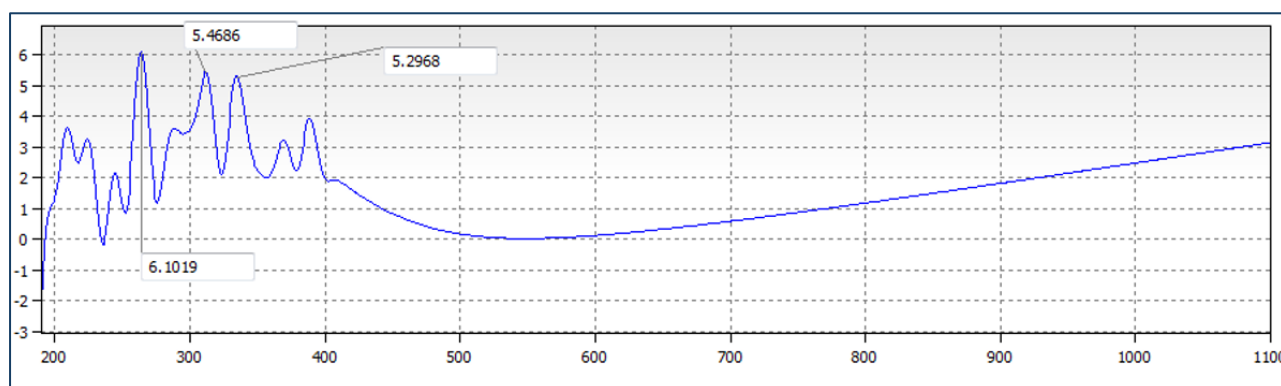


Figure 12 UV-Vis absorption versus wavelength graph of gold nanostars with a broad absorbance peak at 664nm

4.6 Antibacterial Assay:

Significant results of disc diffusion assay of chitosan hydrogel, CAC hydrogel, CAVC hydrogel, and vancomycin were observed against *S. aureus* and *E. coli*.

4.6.1 Antibacterial Activity Against *E. coli*:

Antibacterial Activity of against <i>E. coli</i>	Diameter of Zone of Inhibition(cm)	Average diameter of Zone of Inhibition(cm)
CAVC hydrogel	0, 0.8	0.4
CAC hydrogel	1.4, 1.6	1.5
Chitosan hydrogel	1, 0.9, 0.8	0.9
CNs	0	0

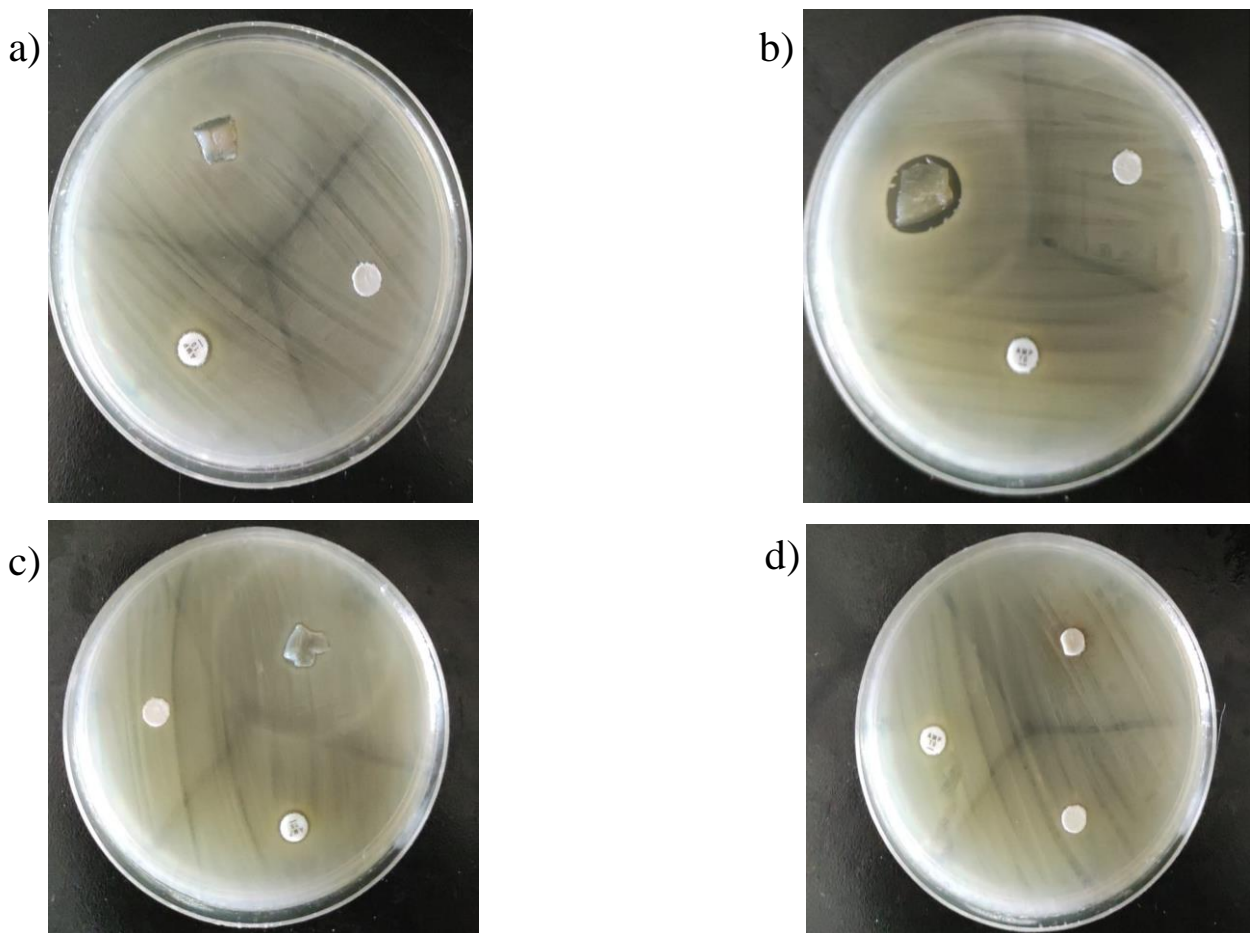


Figure 13 a) Antibacterial Activity of CAVC hydrogel against *E. coli*. b) Antibacterial Activity of CAC hydrogel against *E. coli*. c) Antibacterial Activity of chitosan hydrogel against *E. coli*. d) Antibacterial Activity of CNs against *E. coli*

4.6.2 Antibacterial Activity Against *S. aureus*:

Antibacterial Activity of against <i>S. aureus</i> .	Diameter of Zone of Inhibition(cm)	Average diameter of Zone of Inhibition(cm)
CAVC hydrogel	1.6	1.6
CAC hydrogel	4.1, 4	4.05
Chitosan hydrogel	4.2	4.2
CNs	2.2, 1.7	1.95

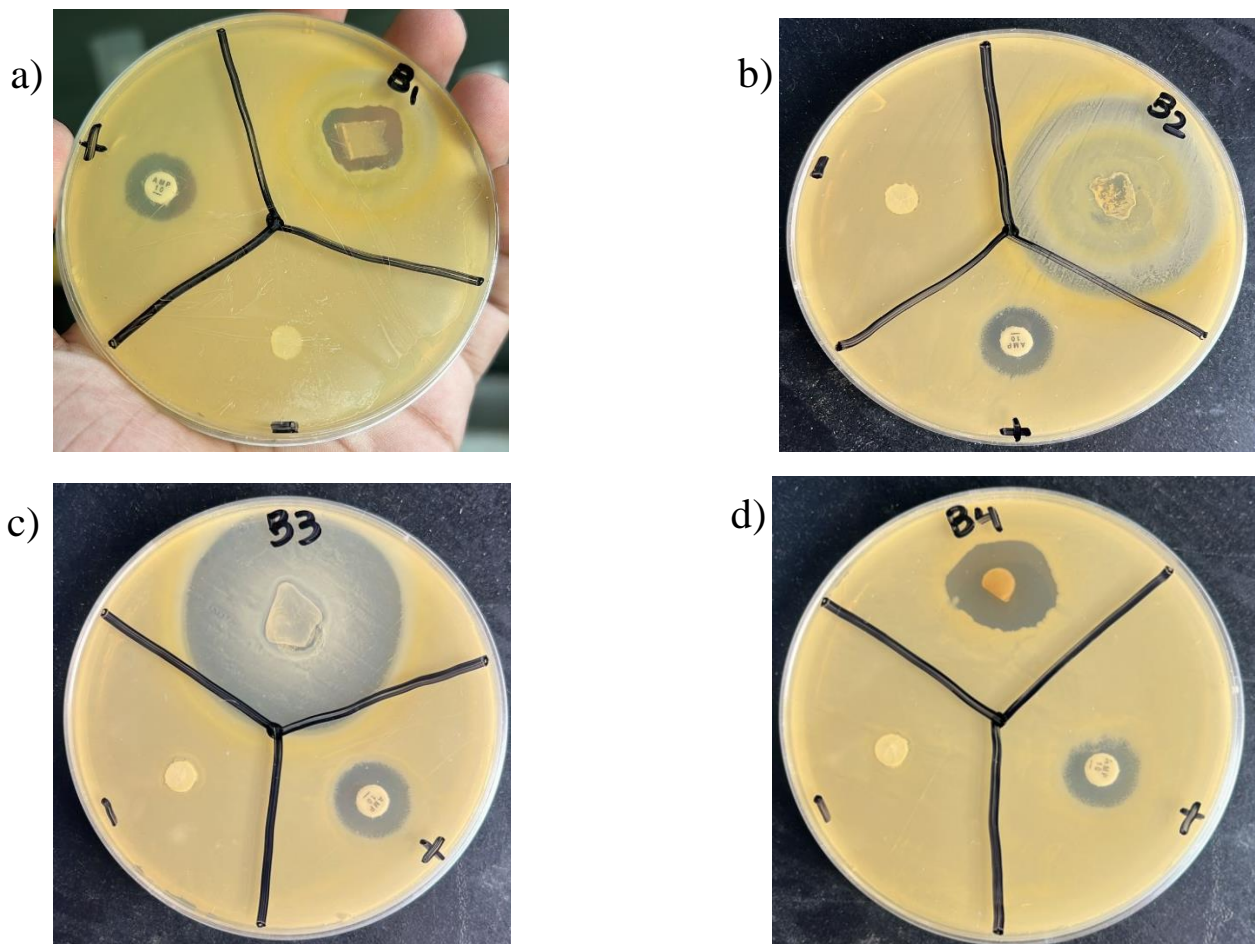


Figure 14 a) Antibacterial Activity of CAVC hydrogel against *S. aureus*. b) Antibacterial Activity of CAC hydrogel against *S. aureus*. c) Antibacterial Activity of chitosan hydrogel against *S. aureus*. d) Antibacterial Activity of CNs against *S. Aureus*.

4.7 Swelling and Degradation Studies:

The swelling study results are presented. Investigating the impact of Carbon nanodots of PHM3 concentration, the swelling ratio of the CMC/Carbon nanodots of PHM3 nanocomposite hydrogels rose with increasing Carbon nanodots of PHM3 content. Introducing nanoparticles can establish physical barriers within the hydrogel network, impeding the unrestricted movement of polymer chains. This constraint leads to a denser packing of polymer chains within the hydrogel. Consequently, when water is absorbed, the heightened density restricts the expansion of the hydrogel compared to its expansion in the absence of nanoparticles. As a result, the swelling ratio increases as the hydrogel retains more water within its constrained network structure.

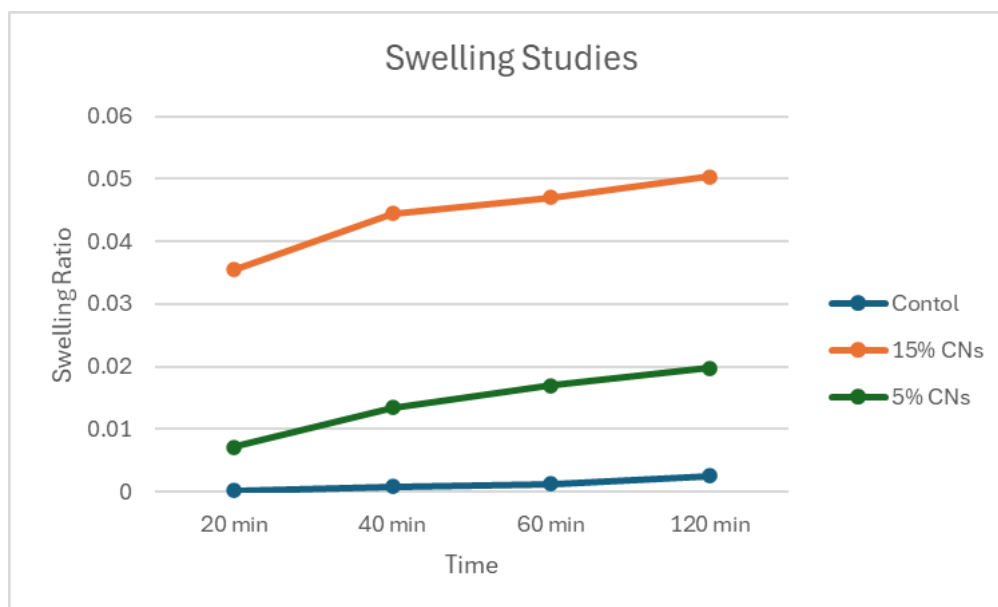


Figure 15 Results from swelling studies

It was noted that reducing the Carbon nanodots of PHM3 content resulted in an increase in the biodegradation of the nanocomposite. The presence of nanoparticles modifies the hydrogel's accessibility to biodegrading agents, including enzymes or environmental elements. Nanoparticles can serve as physical obstacles, protecting the polymer chains from enzymatic degradation or breakdown caused by environmental factors. This protective role slows down the degradation process, leading to a decrease in the biodegradation rate as the nanoparticle concentration rises within the hydrogel.

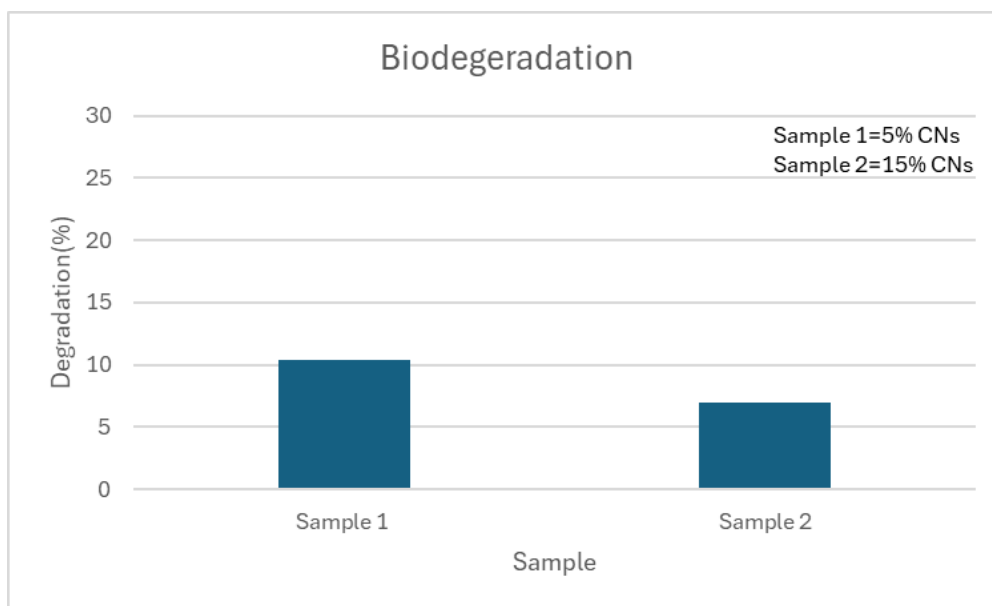


Figure 16 Results from degradation studies

4.8 Drug Delivery Studies:

The release of vancomycin from chitosan hydrogel-based nanoparticles was examined at two distinct pH levels, specifically pH 2 and 7.4, maintaining a temperature of $37^{\circ}\text{C} \pm 0.5$.

4.8.1 Drug Loading (%):

The hydrogels, which included carbon nanodots at 15% and 30% concentrations, were immersed in a 20 mL water-based solution containing 5 mg/mL of vancomycin before their pH-responsive properties were studied. By comparing the hydrogels' weights before and after drug loading, we were able to evaluate their drug loading capabilities. Each film sample underwent this experiment three times to ensure the findings could be reproduced. It was found that CAVC (30%) had a drug loading capacity of 50.06% and CAVC (15%) had a capacity of 19.73%. Carbon nanoparticles and chitosan hydrogel have a synergistic effect, which may explain why the PHM3 Carbon nanodots-coated CA film is so effective in loading drugs. This phenomenon is mainly caused by the increased hydrogen bonding between the surface-attached carbon nanodots' hydroxyl (OH), amino (NH₂), and carboxyl (COOH) groups and the chitosan film's porosity structure. Carbon nanodots, when added to the CA hydrogel sheet, greatly enhanced the chitosan hydrogel's absorption capacity.

4.8.2 Standard Curve of Vancomycin:

A calibration standard curve comprising ten points was constructed, encompassing known drug concentrations ranging from 5 to 0.25 mg/ml. Each sample was analyzed in a UV spectrophotometer at the specific wavelength of 281nm. The entire experiment was conducted in triplicate, and three independent measurements were taken to establish the mean value for drawing the standard curve. A notably linear relationship was observed between the known drug concentrations and their corresponding absorbance values. The linear curve yielded the following results: $y = 0.0061x + 0.0265$, with an R^2 value of 0.9377.

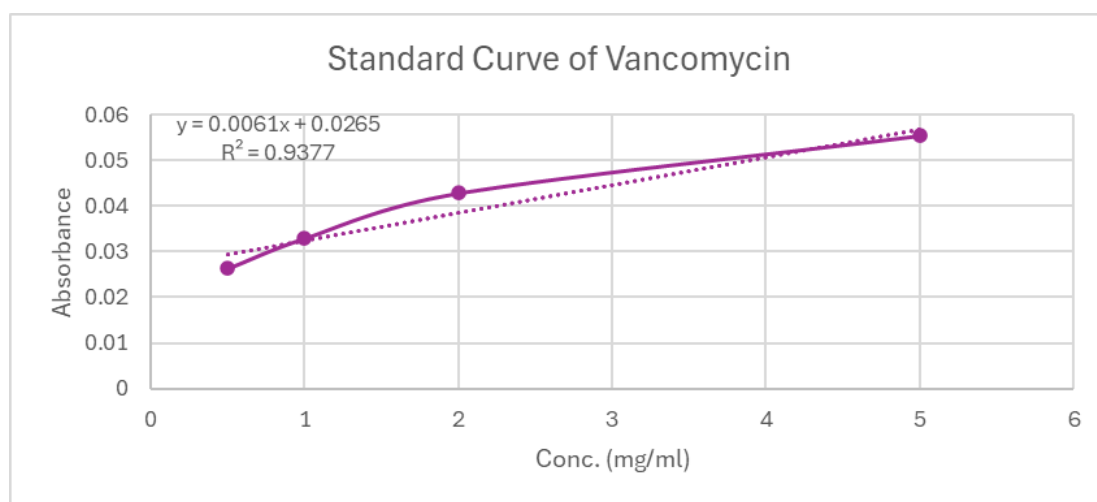


Figure 17 Standard curve of vancomycin

The hydrogel was submerged in 30 mL of double-distilled water to analyze its release profiles. UV-visible spectroscopic measurements were performed by extracting 1 mL aliquots from the release medium at specified intervals, which were subsequently diluted threefold. To ensure a consistent volume of the release medium, 1 mL of fresh medium was replenished after each sampling. The percentage cumulative release of vancomycin (VA) from CAVC hydrogels was assessed by measuring UV-visible absorption at a wavelength approximately 281 nm for each sample.

4.8.3 Drug release profile at pH 7.4

The release of Vancomycin at pH 7.4 was notably slower compared to other pH values, likely due to the presence of nanoparticles in the hydrogel, which facilitated continuous and controlled drug diffusion. Within the initial 20 minutes, only 7.1% of the vancomycin was released from the nanoparticles. Subsequently, after one hour, the release increased to 15.3% from the carbon nanodots. Following this initial slow and gradual release, a maximum release of vancomycin at pH 7.4 was recorded at 30.7% after 48 hours.

4.8.4 Drug release profile at pH 2.0

Regarding the drug release profile at pH 2.0, in contrast to the release rate at pH 7.4, the release of vancomycin from nanoparticles at pH 2.0 was continuous, controlled, and notably higher. The stability of nanoparticles at this pH contributed to the higher release rate. Approximately 41.3% of the drug was released within the first hour, gradually increasing up to the 48th hour. The maximum drug release at pH 2.0 reached 79.3%. These results suggest that approximately 9-10% of the drug remained within the nanoparticles and would be gradually released over time.

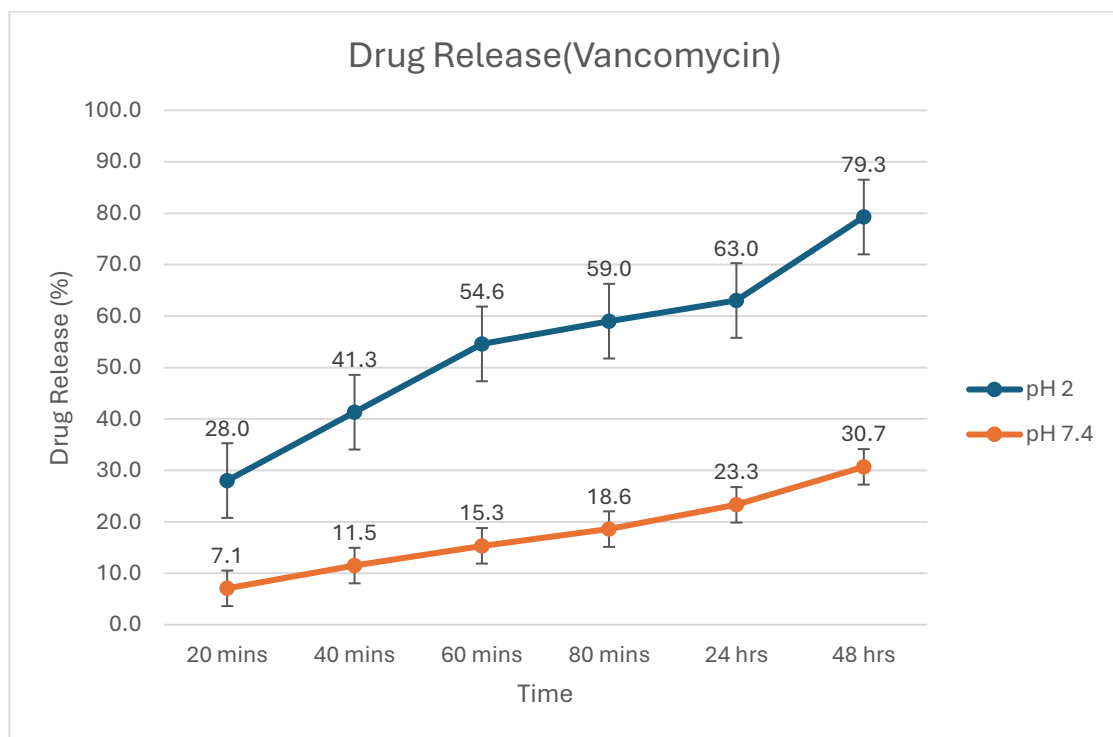


Figure 18 Drug release curve for vancomycin at two different pH levels

FUTURE PROSPECTS

- Cytotoxicity evaluations of both nanoparticles and hydrogels can be conducted both in-vivo and in-vitro so that further applications could be studied for animal and humans.
- MTT Assay can be conducted on cell lines to study anticancer properties of carbon dots and chitosan hydrogel alone (and in conjugation) as well as their drug loading and release properties when used with anticancer drugs.
- Drug release properties of hydrogel and nanoparticles in combination on animal models and in humans. Desirable results can help find advancements in bandage making and drug delivery through wounded sight for quick healing.
- Testing for antibiofilm activity of carbon dots and chitosan hydrogel against resistant biofilm forming bacteria like *Staphylococcus aureus* that are difficult to eradicate once they form biofilm. Also, antibiofilm activity can be checked in conjugation with drugs.
- Functional groups of both hydrogel and carbon dots can be studied further for devising possible methods for incorporating hydrophobic drugs with them.
- The antimicrobial activity of carbon dots as well as chitosan hydrogel can also provide its applications in fresh fruit packaging to improve shelf life and decrease loss due to spoilage. Further advancements include its use in other types of food packaging like ‘Polyethylene terephthalate’ packaging in case of milk and some other products.
- Conjugation of carbon dots with antimicrobial peptides can also be studied and potential applications can be derived from such conjugations.
- Antifungal activity of both gel and carbon dots can be studied alone and in conjugation with each other as well as in conjugation with other antifungal compounds.
- Imaging properties of the carbon dots can also be studied for cancer cell lines while also studying their uptake by cancer cell lines.

BIBLIOGRAPHY

- Achyut Konwar, N. G. (2015). *Green chitosan–carbon dots nanocomposite hydrogel film with superior properties*. Carbohydrate Polymers, Volume 115, 22 January 2015, Pages 238-245.
- Devaraj Bharathi, R. R. (2023). *Green synthesis of chitosan/silver nanocomposite using kaempferol for triple negative breast cancer therapy and antibacterial activity*. Environ Res: 2023 Dec 1;238(Pt 1):117109. doi: 10.1016/j.envres.2023.117109. Epub 2023 Sep 9.
- Ibrahim A Aljuffali 1, M. K. (2023). Development of Gefitinib-Loaded Solid Lipid Nanoparticles for the Treatment of Breast Cancer: Physicochemical Evaluation, Stability, and Anticancer Activity in Breast Cancer (MCF-7) Cells. *Pharmaceuticals (Basel)*, 2023 Nov 2;16(11):1549. doi: 10.3390/ph16111549.
- Josef Jampilek, K. K. (2021). *Advances in Drug Delivery Nanosystems Using Graphene-Based Materials and Carbon Nanotubes*. Materials (Basel). 2021 Mar; 14(5): 1059. Published online 2021 Feb 24. doi: 10.3390/ma14051059.
- Konwar, A., Gogoi, N., Majumdar, G., & Chowdhury, D. (2015). *Green chitosan-carbon dots nanocomposite hydrogel film with superior properties*. In Carbohydrate polymers 115, pp. 238–245. DOI: 10.1016/j.carbpol.2014.08.021. <https://www.s>
- Li, Y. L. (2024). *Encapsulation of Antarctic krill oil and kaempferol co-loaded nano-liposomes in alginate-chitosan hydrogel beads: improved stability and modified digestive behaviour*. International Journal of Food Science & Technology.
- Mishal A., M. I. (2019). *Hydrothermal synthesis of carbon nanodots from bovine gelatin and PHM3 microalgae strain for anticancer and bioimaging applications*. Nanoscale advances.
- Nairah Noor, F. J. (2023). *Nutraceutical and toxicological evaluation of hydrogels architected using resistant starch nanoparticles and gum acacia for controlled release of kaempferol*. Food Structure, Volume 35, January 2023, 100307.

- Niladri Sarkar, G. S. (2017). *Carbon quantum dot tailored calcium alginate hydrogel for pH responsive controlled delivery of vancomycin*. European Journal of Pharmaceutical Sciences, Volume 109, 15 N.
- Rasul Rakhshaei, H. N. (2019). *Graphene quantum dot cross-linked carboxymethyl cellulose nanocomposite hydrogel for pH-sensitive oral anticancer drug delivery with potential bioimaging properties*. Int J Biol Macromol 2020 1:150:1121-1129.
- Ru Feng, L. W. (2020). *Development of the pH responsive chitosan-alginate based microgel for encapsulation of Juglans regia L. polyphenols under simulated gastrointestinal digestion in vitro*. Carbohydrate Polymer, 2020 Dec 15:250:116917. doi: 10.1016/j.carbpol.2020.116917. Epub 2020 Aug 15.
- Samina Nazir, M. U. (2021). *Nanocomposite Hydrogels for Melanoma Skin Cancer care and Treatment: In-vitro drug delivery, drug release kinetics and anti-Cancer activities*. Arabian Journal of Chemistry 14(2):103120.
- Simpson, Aaron, R. R. Pandey, Charles C. Chusuei, Kartik Ghosh, Rishi Patel, and Adam K. Wanekaya. "Fabrication characterization and potential applications of carbon nanoparticles in the detection of heavy metal ions in aqueous media." Carbon 127 (2018): 122-130.
- Sawant, V. J., Bamane, S. R., Kanase, D. G., Patil, S. B., & Ghosh, J. S. (2016). Encapsulation of curcumin over carbon dot coated TiO₂ nanoparticles for pH sensitive enhancement of anticancer and anti-psoriatic potential. <https://doi.org/10.1039/c6ra13851a>
- Hines DA, Kamat PV. Recent advances in quantum dot surface chemistry. ACS Appl Mater Interfaces. 2014 Mar 12;6(5):3041-57. doi: 10.1021/am405196u. Epub 2014 Feb 17. PMID: 24506801.
- Zuo P, Haberer LJ, Fang L, Hunt TL, Ridgway D, Russo MW. Integration of modeling and simulation to support changes to ondansetron dosing following a randomized, double-blind, placebo-, and active-controlled thorough QT study. J Clin Pharmacol. 2014 Nov;54(11):1221-9. doi: 10.1002/jcph.322. Epub 2014 May 6. PMID: 24782199.
- Dong K, Du Y, Rinkevich F, Nomura Y, Xu P, Wang L, Silver K, Zhorov BS. Molecular biology of insect sodium channels and pyrethroid resistance. Insect Biochem Mol Biol.

2014 Jul;50:1-17. doi: 10.1016/j.ibmb.2014.03.012. Epub 2014 Apr 3. PMID: 24704279; PMCID: PMC4484874.

Zuo, P., Xiao, D., Gao, M., Peng, J., Pan, R., Xia, Y., & He, H. (2014). Single-step preparation of fluorescent carbon nanoparticles, and their application as a fluorometric probe for quercetin. *Microchimica Acta*, 181(11–12), 1309–1316. <https://doi.org/10.1007/s00604-014-1236-3>

Li X, Liu W, Sun L, Aifantis KE, Yu B, Fan Y, Feng Q, Cui F, Watari F. Effects of physicochemical properties of nanomaterials on their toxicity. *J Biomed Mater Res A*. 2015 Jul;103(7):2499-507. doi: 10.1002/jbm.a.35384. Epub 2014 Dec 19. PMID: 25530348.

Sun YP, Zhou B, Lin Y, Wang W, Fernando KA, Pathak P, Meziani MJ, Harruff BA, Wang X, Wang H, Luo PG, Yang H, Kose ME, Chen B, Veca LM, Xie SY. Quantum-sized carbon dots for bright and colorful photoluminescence. *J Am Chem Soc*. 2006 Jun 21;128(24):7756-7. doi: 10.1021/ja062677d. PMID: 16771487.

Kasibabu, B. S. B., D'souza, S. L., Jha, S., Singhal, R. K., Basu, H., Kailasa, S. K., ... Liu, G. (2015). One-step synthesis of fluorescent carbon dots for imaging bacterial and fungal cells. *Anal. Methods*, 7(6), 2373–2378. <https://doi.org/10.1039/C4AY02737J>

Das, P., Bose, M., Ganguly, S., Mondal, S., Das, A. K., Banerjee, S., & Das, N. C. (2017). Green approach to photoluminescent carbon dots for imaging of gram-negative bacteria *Escherichia coli*. *Nanotechnology*, 28(19). <https://doi.org/10.1088/1361-6528/aa6714>

Esteves da Silva, J. C. G., & Gonçalves, H. M. R. (2011). Analytical and bioanalytical applications of carbon dots. *TrAC - Trends in Analytical Chemistry*, 30(8), 1327–1336. <https://doi.org/10.1016/j.trac.2011.04.009>

Sachdev, A., Matai, I., & Gopinath, P. (2016). Carbon dots incorporated polymeric hydrogels as multifunctional platform for imaging and induction of apoptosis in lung cancer cells. *Colloids and Surfaces B: Biointerfaces*, 141, 242–252. <https://doi.org/10.1016/j.colsurfb.2016.01.043>

Hsu, P.-C., Chen, P.-C., Ou, C.-M., Chang, H.-Y., & Chang, H.-T. (2013b). Extremely high inhibition activity of photoluminescent carbon nanodots toward cancer cells. *Journal of Materials Chemistry B*, 1(13), 1774. <https://doi.org/10.1039/c3tb00545>

Mohd Sameer, Yaseera Arif, Anjlina Aqil, Arif Nadaf, Km Rafiya, Nazeer Hasan, Prashant Kesharwani, Farhan Jalees Ahmad, Carbon nanodots as a remedial nanovesicles for drug delivery, European Polymer Journal, <https://doi.org/10.1016/j.eurpolymj.2023.112515>.

Narayan Bhattarai, Jonathan Gunn, Miqin Zhang, Chitosan-based hydrogels for controlled, localized drug delivery, Advanced Drug Delivery Reviews, <https://doi.org/10.1016/j.addr.2009.07.019>.

Cheng, X., Xie, Q., & Sun, Y. (2023). Advances in nanomaterial-based targeted drug delivery systems. *Frontiers in bioengineering and biotechnology*, 11, 1177151

ORIGINALITY REPORT

10%

SIMILARITY INDEX

7%

INTERNET SOURCES

7%

PUBLICATIONS

1%

STUDENT PAPERS

PRIMARY SOURCES

1

www.ncbi.nlm.nih.gov

Internet Source

2%

2

Bhattacharai, N.. "Chitosan-based hydrogels for controlled, localized drug delivery", *Advanced Drug Delivery Reviews*, 20100131

Publication

1%

3

www.mdpi.com

Internet Source

1%

4

Sania Arif, Aamina Batool, Nauman Khalid, Iftikhar Ahmed, Hussnain Ahmed Janjua. "Comparative analysis of stability and biological activities of violacein and starch capped silver nanoparticles", *RSC Advances*, 2017

Publication

<1%

5

Achyut Konwar, Neelam Gogoi, Gitanjali Majumdar, Devasish Chowdhury. "Green chitosan-carbon dots nanocomposite hydrogel film with superior properties", *Carbohydrate Polymers*, 2015

Publication

<1%

6	Mishal Amjad, Maheen Iqbal, Amir Faisal, Arshad Mahmood Junjua et al. "Hydrothermal synthesis of carbon nanodots from bovine gelatin and PHM3 microalgae strain for anticancer and bioimaging applications", <i>Nanoscale Advances</i> , 2019 Publication	<1 %
7	Submitted to University of Sunderland Student Paper	<1 %
8	S. Sood, Vinod Kumar Gupta, Shilpi Agarwal, Kamal Dev, Deepak Pathania. "Controlled release of antibiotic amoxicillin drug using carboxymethyl cellulose-cl-poly(lactic acid-co-itaconic acid) hydrogel", <i>International Journal of Biological Macromolecules</i> , 2017 Publication	<1 %
9	Submitted to University of Greenwich Student Paper	<1 %
10	Lana Glerieide Silva Garcia, Maria Gleiciane da Rocha, Laysa Rocha Lima, Arcelina Pacheco Cunha et al. "Essential oils encapsulated in chitosan microparticles against <i>Candida albicans</i> biofilms", <i>International Journal of Biological Macromolecules</i> , 2021 Publication	<1 %
11	pubs.rsc.org Internet Source	<1 %

12	sutir.sut.ac.th:8080 Internet Source	<1 %
13	Submitted to University of Northumbria at Newcastle Student Paper	<1 %
14	Ming-Chao Jiang, Hong-Bing Liu, Jia-Qi Wang, Shuang Li, Zhi Zheng, Dun Wang, Hua Wei, Cui-Yun Yu. "Optimized Aptamer Functionalization for Enhanced Anticancer Efficiency in Vivo", International Journal of Pharmaceutics, 2022 Publication	<1 %
15	ijpsr.com Internet Source	<1 %
16	www.researchgate.net Internet Source	<1 %
17	Submitted to University of Auckland Student Paper	<1 %
18	Submitted to University of Ulster Student Paper	<1 %
19	mdedge-cache.qa00.mdedge.com Internet Source	<1 %
20	Long, Jinlin, Xiuqiang Xie, Jie Xu, Quan Gu, Liming Chen, and Xuxu Wang. "Nitrogen-Doped Graphene Nanosheets as Metal-Free	<1 %

Catalysts for Aerobic Selective Oxidation of Benzylic Alcohols", ACS Catalysis, 2012.

Publication

21	oaktrust.library.tamu.edu Internet Source	<1 %
22	www.nature.com Internet Source	<1 %
23	discovery.researcher.life Internet Source	<1 %
24	fsc.esn.ac.lk Internet Source	<1 %
25	link.springer.com Internet Source	<1 %
26	Deming Dong, Tianjiao Liu, Dapeng Liang, Xipeng Jin, Zihan Qi, Anfeng Li, Yang Ning. "Facile Hydrothermal Synthesis of Chlorella-Derived Environmentally Friendly Fluorescent Carbon Dots for Differentiation of Living and Dead Chlorella", ACS Applied Bio Materials, 2021 Publication	<1 %
27	Rahul S. Tade, Pravin O. Patil. "Theranostic Prospects of Graphene Quantum Dots in Breast Cancer", ACS Biomaterials Science & Engineering, 2020 Publication	<1 %

28	d.docksci.com Internet Source	<1 %
29	ojs.acad-pub.com Internet Source	<1 %
30	Baruah, Upama, Neelam Gogoi, Gitanjali Majumdar, and Devasish Chowdhury. "β-Cyclodextrin and calix[4]arene-25,26,27,28-tetrol capped carbon dots for selective and sensitive detection of fluoride", <i>Carbohydrate Polymers</i> , 2015. Publication	<1 %
31	Kathirvel Brindhadevi, T.P. Kim, Mathiyazhagan Narayanan, Arunachalam Chinnathambi, Jintae Lee, Devaraj Bharathi. "Evaluation of Zn-Cd-Sn-S nanostructures for in vitro pyrene degradation and antimicrobial activity", <i>Environmental Research</i> , 2024 Publication	<1 %
32	Qiuyan Luo, Xiaohui Huang, Yong Luo, Hanmeng Yuan, Tingting Ren, Xianjun Li, Dong Xu, Xin Guo, Yiqiang Wu. "Fluorescent chitosan-based hydrogel incorporating titanate and cellulose nanofibers modified with carbon dots for adsorption and detection of Cr(VI)", <i>Chemical Engineering Journal</i> , 2021 Publication	<1 %
33	datapdf.com Internet Source	

		<1 %
34	e-space.mmu.ac.uk Internet Source	<1 %
35	eprints.kfupm.edu.sa Internet Source	<1 %
36	mts.intechopen.com Internet Source	<1 %
37	psaspb.upm.edu.my Internet Source	<1 %
38	tudr.thapar.edu:8080 Internet Source	<1 %
39	Meng Li, Quanyu Shi, Ningxin Song, Yumeng Xiao, Lidong Wang, Zhijun Chen, Tony D. James. "Current trends in the detection and removal of heavy metal ions using functional materials", <i>Chemical Society Reviews</i> , 2023 Publication	<1 %
40	Rashmita Das, Rajib Bandyopadhyay, Panchanan Pramanik. "Carbon quantum dots from natural resource: A review", <i>Materials Today Chemistry</i> , 2018 Publication	<1 %
41	Deepak Pathania, Sarita Kumari. "Nanocomposites Based on Biopolymer for	<1 %

Biomedical and Antibacterial Applications",
American Chemical Society (ACS), 2020

Publication

42

Jun Hu, Jiangping Guo, Junyan Zhao, Zixun Chen, Mulenga Kalulu, Gaojian Chen, Guodong Fu. "Multifunctional, Degradable Wearable Sensors Prepared with an Initiator and Cross-Linker-Free Method", ACS Applied Materials & Interfaces, 2024

Publication

<1%

Exclude quotes Off

Exclude matches Off

Exclude bibliography Off